EXPERIMENTAL MEASUREMENT OF STEAM-WATER RELATIVE PERMEABILITY

A REPORT SUBMITTED TO
THE DEPARTMENT OF PETROLEUM ENGINEERING
STANFORD UNIVERSITY
IN PARTIAL FULFILLMENT OF THE REQUIREMENTS
FOR THE DEGREE OF MASTER OF SCIENCE

Glenn F. Mahiya

July 1999

I certify that I have read this report and that in my opinion it is fully adequate, in scope and in quality, as partial fulfillment of the degree of Master of Science in Petroleum Engineering.

Dr. Roland N. Horne
(Principal advisor)

Abstract

Relative permeability curves for two-phase flow of water in a porous medium have been obtained from a series of steady state experiments using an approach that minimizes most of the uncertainties associated with such measurements, especially in pressure, heat loss and saturation. The use of heat guards with an automatic control system made it possible for the experiments to proceed under near-adiabatic conditions that allowed the existence of flat-saturation regions favored in relative permeability calculations. X-ray computer tomography (CT) aided by measuring in-situ steam saturation more directly.

The measured steam-water relative permeability curves assume a shape similar to those obtained by Corey (1954) for the simultaneous flow of nitrogen and water. The close agreement between the curves by Satik (1998) and this study establishes the reliability of the experimental method and instrumentation adopted in both investigations, at least in terms of reproducibility of results.

This study likewise suggests that the effect of slippage in the steam phase is of significance even in two-phase water flow. Corrections for this effect need to be made in order to obtain relative permeability values that are standardized with respect to pressure.

Acknowledgment

This research was conducted with financial support through the Stanford Geothermal Program under **Department of Energy Grant No. DE-FG07-95ID13370**.

The contributions of the following individuals are much appreciated: **Dr. Cengiz Satik**, for his guidance in the experimental details of the research and for laying the foundations of the work; **Dr. Kewen Li**, for his insightful suggestions; **Ms. Huda Nassori**, for her invaluable assistance in the laboratory. Most of all, I thank my advisor, **Dr. Roland Horne**, for patiently providing direction and motivation in the course of this research work.

I whole-heartedly dedicate this work to my parents and sisters who inspire and support me unconditionally, and above all, to the Almighty Father for His greater glory.

Table of Contents

1 Introduction

Fluid flow in porous media is typically modeled using Darcy's law. As an extension to simultaneous flow of multiple phases, the concept of relative permeability is used to account properly for the flow behavior of one phase in the presence of the others. Relative permeability has significant impact on the prediction of reservoir performance and, thus, merits much attention from experimentalists and practitioners in the field of reservoir engineering.

Relative permeability is believed to depend primarily on the volume occupied by a particular phase and has, thus, been expressed mainly as a function of saturation since its introduction by Buckingham in 1907. While relative permeability relations for oil-water and oil-gas flow are well-known for many applications in petroleum engineering, similar curves for steam and water have not been fully established. The more commonly used forms of relative permeability curves are those of Corey (1954) and the simpler linear or X-type of relations. Efforts toward obtaining such curves range from field-based theoretical studies using well test data or production histories, to laboratory scale experiments involving injection of fluid into either an artificial porous medium or actual rock core or plug. Models based on field data (Grant, 1977; Horne and Ramey, 1978; Sorey et al., 1980) suffer from the assumption that the reservoir is strictly a porous medium when in reality most reservoirs, especially geothermal reservoirs, are fracture-dominated. Furthermore, in-situ saturation is grossly estimated from production enthalpy and averaged fieldwide.

Laboratory experiments offer better control of parameters relevant to the determination of relative permeability and, thus, give more reliable results. Unsteady state methods where the state of the system varies with time are limited by the assumptions used in the analyses. Steady state experiments, on the other hand, wait until the flow of injected fluid is time-invariant before measurements are made. Many past experiments, however, suffered from capillary end effects that complicate the interpretation of data.

Furthermore, obtaining saturations has posed a challenging task. Indirect measurements based on thermodynamic properties and oil-water relative permeability curves have been attempted (Arihara, 1976). Recovery time of chemical tracer injected with the fluid was also tried (Sanchez, 1988) but such a technique ignores spatial variation of saturation over the entire core and capillary end-effects at low flow rates. Direct measurements of liquid saturation was first tried by Chen (1976) using a capacitance probe, and later used by Counsil and Ramey (1979) in their studies of steam-water boiling flow. Gamma-ray densitometers were used in experiments with artificial sandpacks (Verma, 1986) but equipment problems led to the investigation of only a limited part of the relative permeability curves. Piquemal (1994) used a similar instrument on an uncosolidated pack and obtained results that differ from those of Verma (1986).

The use of computer-aided tomography (CT) in steam saturation measurements was introduced by Clossman and Vinegar (1988) in their steam-water experiment with cores from oil fields at residual oil saturation. However, end-effects which are significant for the dimensions of the core and flow rates used in the experiments were not considered in the study, and the temperature distribution along the core was only assumed instead of measured.

Significant advances in experimental design were achieved by Ambusso (1996) using X-ray CT scanning and real-time measurement of pressures, temperatures and heat fluxes along the core. Two different methods were used for low and high steam saturations. For low fluid enthalpy (i.e., low steam saturation), a modification to the method used by Arihara (1976) was applied. A mixture of separate liquid and streams was used for the second method applied to cases of higher steam saturation. The experiments by Ambusso (1996) yielded linear-type relative permeability curves. This study served as precursor for succeeding experiments that constantly improved on specific aspects of the apparatus. Satik (1998) used a very similar setup injecting hot water and slightly superheated steam at varying proportions to achieve two-phase conditions in the core.

The study that we discuss in this report built upon the works of Ambusso (1996) and Satik (1998) and aims to improve on experimental techniques especially in terms of minimizing the uncertainty of heat loss measurements that are important in the calculations of steam-water relative permeability.

2 Theoretical Background

The idea behind relative permeability stems from the fact that fluid behaves differently when it is flowing together with a different fluid. The situation is even more complicated in the case of steam and water since one phase can readily be transformed to the other and hence, the mass flux of each phase is not constant. Nevertheless, the theoretical foundations of liquid-vapor relative permeability are still applicable if these phase exchanges are taken into account.

In this chapter, we look into the equations that are relevant in establishing the desired steam-water relative permeability curves from steady-state flow-through experiments such as those conducted for this study.

2.1 Relative permeability equations

Single phase flow in a porous medium is typically governed by Darcy's law relating the fluid velocity, u, to the pressure drop, Δp, over the distance, ΔL; the viscosity, μ, and; the absolute permeability, k, of the medium as in Equation 2.1.

$$u = \frac{k}{\mu}\frac{\Delta p}{\Delta L} \tag{2.1}$$

Considering the flow of liquid and vapor phases in a two-phase mixture and taking into account relative permeability, k_r, gives the following, Darcy's law may be expressed in terms of mass flow rate, m, as

$$m_s = \frac{kk_{rs} A \rho_s}{\mu_s} \frac{\Delta p}{\Delta L} \tag{2.2a}$$

$$m_w = \frac{kk_{rw} A \rho_w}{\mu_w} \frac{\Delta p}{\Delta L} \tag{2.2b}$$

where the fluid density is denoted by ρ and the cross-sectional area of the porous medium is A. The subscript w identifies the liquid water phase while s pertains to the steam or vapor phase. These equations can then be rearranged to give the expressions for relative permeability:

$$k_{rs} = \frac{x m_t \mu_s}{\rho_s k A} \frac{\Delta L}{\Delta p} \tag{2.3a}$$

$$k_{rw} = \frac{(1 - x) m_t \mu_w}{\rho_w k A} \frac{\Delta L}{\Delta p} \tag{2.3b}$$

where the mass flow rates have been expressed in terms of the steam mass fraction, x, and the total mass flowrate, m_t.

2.2 Calculation of mass flow rates

The parameters that appear in the equations for relative permeability may be obtained easily from steady-state experiments with the exception of mass flow rate. As mentioned earlier, the exchange of mass between phases complicates the determination of in-situ flow rate. To estimate this parameter a careful accounting of energy is required. Consider the flow of two-phase water in a core between two points labeled 1 and 2 as shown in Figure 2.1.

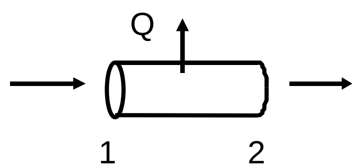

Figure 2.1: Simple diagram of a core segment for mass and energy balance.

At steady-state, continuity of mass and energy requires that Equations 2.4 and 2.5 be satisfied. Here, h denotes the specific enthalpy of a phase, Q_{12} is the heat lost from the core, subscripts 1 and 2 identify the conditions prevailing at the two points, and t denotes properties for the combined liquid and vapor streams.

$$m_t = m_{s1} + m_{w1} = m_{s2} + m_{w2} \tag{2.4}$$

$$m_t h_t = m_{s1} h_{s1} + m_{w1} h_{w1} = m_{s2} h_{s2} + m_{w2} h_{w2} + Q_{12} \tag{2.5}$$

Letting $m_s = x\, m_t$ and $m_w = (1\text{-}x)\, m_t$, Equations 2.4 and 2.5 may be combined to solve for the steam fraction x_2 at point 2 given the dryness x_1 at point 1 and phase enthalpies at these two conditions. The latent heat of vaporization, L, is simply h_s-h_w. Specific enthalpies are obtainable from steam tables given the temperatures and pressures at the two points assuming flat-interface thermodynamics. This analysis can be applied successively between measurement points to obtain mass flow rates as a function of position given the known constant total flow rate and the total energy at the inlet as

$$x_2 = x_1 \frac{L_1}{L_2} + \frac{h_{w1} - h_{w2}}{L_2} - \frac{Q_{12}}{m_t L_2}. \tag{2.6}$$

2.3 Saturation

Finding the in-situ steam saturation proved to be a great challenge for many earlier relative permeability experiments. The use of X-ray computer-aided tomography (CT) has made such measurements more direct and hence, reliable. The CT number is related to the density of the material being scanned, with a higher value indicating a denser composition. Using this concept, the void space or porosity, ϕ, at a given cross-section of the core can be calculated by

$$\phi = \frac{CT_{wet} - CT_{dry}}{CT_{water} - CT_{air}} \tag{2.7}$$

where CT_{wet} is the CT value when the core is fully saturated with water, and CT_{dry} is the value when the core is completely void or evacuated. CT_{water} denotes the CT number for water by itself (equal to 0), while CT_{air} is for air (equal to -1000). When the core is occupied by two-phase water, the steam saturation, S_{st}, and that of water, S_w, can be obtained from the following relation

$$S_{st} = \frac{CT_{hw} - CT_{meas}}{CT_{hw} - CT_{dry}} \tag{2.8a}$$

$$S_w = 1 - S_{st} \tag{2.8b}$$

where CT_{hw} and CT_{meas} are the values when the core is saturated with hot liquid water and two-phase fluid, respectively. Note that it is important to use the value for the hot water scan instead of cold water since there already exists a density change between these two conditions. Using CT_{wet} instead of CT_{hw} would give a steam saturation that is non-zero despite the fact that there is still no steam present during a hot water scan, thus, overestimating steam saturation.

3 Experiment

In this chapter, we discuss in detail the experimental design that will enable measurements of parameters relevant to determining steam-water relative permeability as described in Chapter 2. Several significant modifications have been made in recent years to improve the experimental setup for these steady-state flow-through experiments. An important example was the use of the more reliable core holder made from high temperature plastic instead of from epoxy. The apparatus that generates hot water and steam for the inlet has also evolved from bulky furnaces to convenient in-situ heaters. Data acquisition in itself demonstrates how increasingly sophisticated and complex the experiment became. These and other minor enhancements represent the desire to continuously improve the techniques and ensure the reliability and reproducibility of results.

3.1 Experimental method

The physical parameters required to establish relative permeability curves are pressure, temperature, heat flux and saturation. The preparation involved drying the core by subjecting it to $120^{O}C$ in an oven and simultaneously pulling a vacuum on it. There was no need to bake the core at higher temperatures for the purpose of deactivating clays in the rock since this has been done in past experiments. Once dried, the auxiliary components were assembled as will be described in the next section. A dry X-ray scan was then made to obtain CT_{dry} (defined in Section 2.3). This was followed by fully saturating the core with water and scanning it to obtain $CT_{we,}$., and from these the porosity distribution was obtained. The next step was to flow hot liquid water to obtain CT_{hw} which is necessary for calculating experimental saturations. The completion of this scan marked the start of the actual flow-through experiments. The electrical power into the system was then increased in stages by changing the voltage settings of the heaters that generated dry steam and hot water. Such a heat-up procedure was essentially a displacement of the wetting phase (water) by the non-wetting phase (steam) and hence, is a drainage process. Two-phase flow in the core was then allowed to stabilize before an X-ray scan was performed. At every stage, pressure, temperature and heat fluxes from the core were measured. The maximum steam saturation was reached by injecting only steam at the inlet. Once this was achieved, input power to the steam and water heaters was gradually decreased to implement an imbibition process whereby liquid water displaces steam. The concepts and equations developed in Chapter 2 were applied to regions of flat saturation as identified from the CT scans. Calculated relative permeability to steam and water were then plotted against the saturation measurements to obtain the curves.

3.2 General design

Figure 3.1 is a schematic of the apparatus that allows real-time measurement of these quantities. The main component of the system was a 17-inch Berea sandstone core with a nominal absolute permeability of 1200 md and measured porosity of 24%. This was the same core used in experiments by Satik (1998). Pressure and temperature were measured through ports at eight positions along the core spaced 5 cm. apart. These ports served to connect the core to pressure transducers via plastic tubings, and as tapping points in which thermocouple wires were inserted for temperature readings. The core was enclosed in a core holder that provided a boundary for fluid flow, mechanical support, and thermal insulation to some extent. On one end of the core, a heating head was attached to seal the inlet or upstream end while housing the two heaters that generated hot water and steam. An end cap with provision for fluid exit sealed the downstream end of the core. Heat flux sensors were attached (by high-temperature glue) along the core holder. Controllable flexible heaters completely enveloped the core holder and the heat flux sensors to balance heat losses. A blanket of insulating fiber around this assembly further reduced the escape of heat.

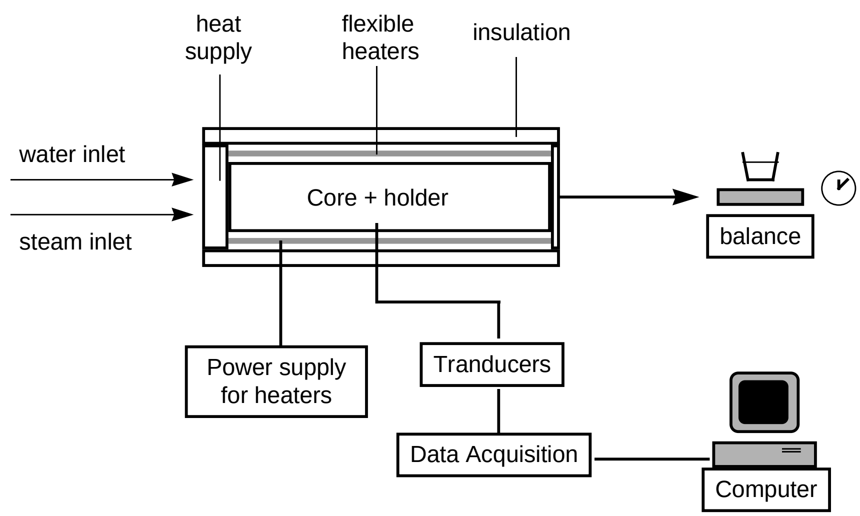

Figure 3.1: Experimental setup for the flow-through experiment using heat guards.

In order to achieve two-phase conditions in the core, dry steam and hot liquid water were injected separately from two streams at the inlet. Each stream of fluid came from deionized water pumped from a common reservoir to a boiler and then to a condensing loop. This process eliminated dissolved air that could introduce errors in saturation measurements. The deaerated water was then delivered to the heating head where each of the two streams was heated to either steam or hot water. Steam and water then became partially mixed at the interface between the core and the head, and further mixed as they entered the porous medium. Fluid exited the core and was directed to the sink where volumetric rate was checked using a graduated cylinder and timer, and compared with the injection rates specified at the pumps.

In-situ saturation were based on images generated by Picker's Synerview 1200X X-ray CT scanner. The core assembly was mounted and secured on a stepper motor that allowed movement of the core in and out of the X-ray's gantry with 1 cm interval. We were able to take measurements at 41 points along the core. Figure 3.2 shows the major components of the experimental setup and the CT scanner.

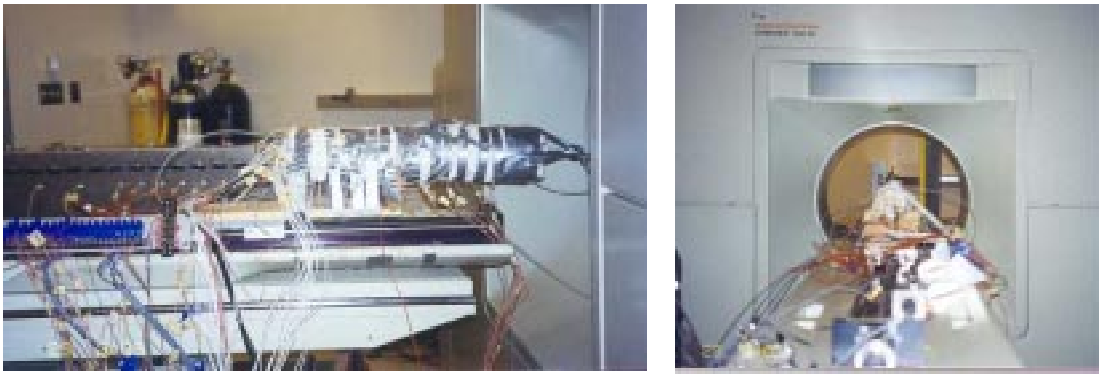

(a) *(b)*

Figure 3.2: (a) Core assembly mounted on stepper motor. White wires from the assembly are for flexible heater while the red wires are for the heat flux sensors. The panel on the left has the terminals for plugging in thermocouple and sensor devices. (b) Core assembly as it moves into the X-ray machine's gantry.

3.3 Flexible heat guard

Despite the thick layer of insulation around the core holder, there was still considerable heat escaping from the core. By supplying the exact amount of heat that was lost back to the system, overall heat loss could be negligible, if not zero. We have designed flexible heaters custom-made for this experiment. Figure 3.3 shows a schematic of one of the Kapton-insulated flexible heaters.

Since single-sheet heaters long enough to completely cover the core system were not available, we used two separate 8"x10" and 9"x10" sheets. Holes with 0.53" diameters were provided to ensure complete contact between the heater and the core holder despite the presence of protruding pressure ports lining the core length. Each sheet was an array of eight or nine 1"x10" strips of heating elements that could be controlled independently. In effect, we had 17 different heaters rated at 2.5 W/in^2 at 115 volts. Since the heaters required only a small amount of current to operate, we used a transformer to step-down the voltage from 120 VAC to 60 VAC. At the end of each strip of heater, two Teflon-insulated wires connected the element to a channel in the data acquisition module and to the power supply. The flexible thin-film heaters did not cause significant interference when subjected to X-ray CT scanning.

This near-adiabatic experiment replaced the nonadiabatic setup used in previous works. Conducting measurements in such an environment eliminates the need to account for heat losses when calculating the relative permeability to water and to steam, and hence, reduces the uncertainty in the values computed. Aside from this, steady-state could be reached more easily with an adiabatic system and, hence, the duration of the experiment can be reduced and more data points can be obtained within the same period of time.

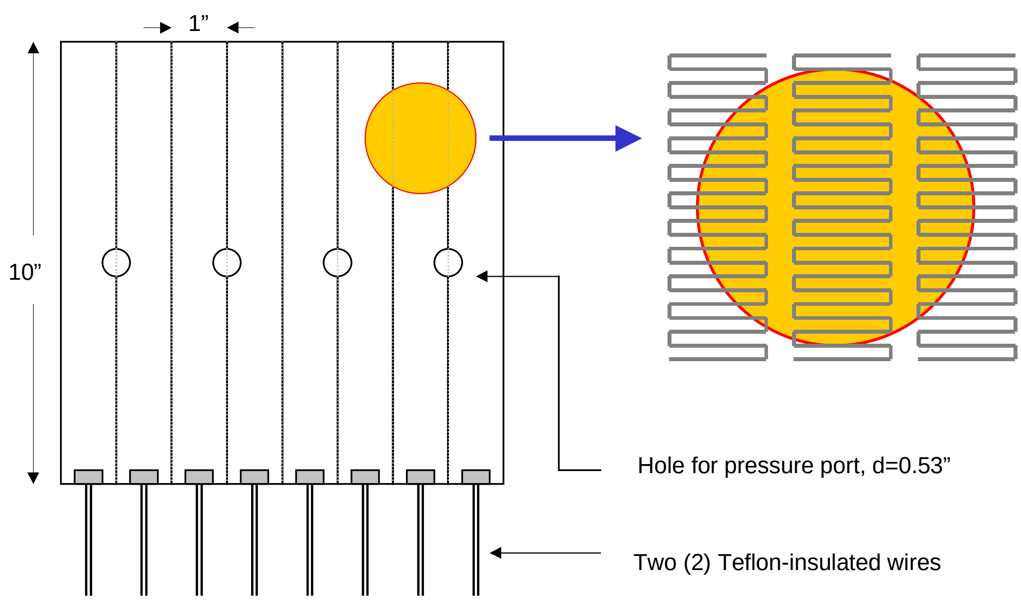

Figure 3.3: Schematic of flexible heaters

3.4 Data acquisition and control system

Pressures, temperatures and heat fluxes were measured continuously with the aid of several National Instruments data acquisition (DAQ) devices. In particular, we used three

(3) SCXI-1100 modules housed in a SCXI-1000 chassis box. Electrical wires transmitting signals from the pressure transducers, thermocouples and heat flux sensors were sent to the DAQ module through channels in the SCXI-1300 terminal blocks. Each terminal block attached to a SCXI-1100 module that conditions the signals and sent them for conversion, display and storage to a personal computer via the parallel port.

To control the individual heating elements, we used National Instruments' SCXI 1163-R module. It consisted of 32-channel optically isolated digital output/solid-state relays that have no moving parts and, hence, are not subject to the limited lifetimes of electromechanical relays. In the closed state, each relay had a maximum resistance of 8 ohms and carried up to 200 mA of current. The SCXI-1326 terminal block was used to connect the heaters to the module installed in the SCXI chassis. Figure 3.4 illustrates how the flexible heaters and the data acquisition module were configured.

Heat flux sensors were positioned between the core holder and the heating blanket to monitor heat loss. These sensors were connected to a separate data acquisition module (SCXI-1100), and the measurements were displayed by the graphical programming software for instrumentation (LABVIEW version 4.1). Automatic control of the heaters to maintain a net flux of zero was likewise achieved through LABVIEW.

Since heat loss varied with distance from the inlet of the core, the heat replenishment would likewise vary accordingly to attain zero net heat flux. Aside from spatial variation, heat loss also changed with time especially in the early part of the experiment when equilibrium had not been reached. Since the SCXI-1163R basically controls a device by switching it on or off, there was no direct way of providing variable power to the heater. It was not feasible to obtain a constant output from the heater that was different from the maximum it could deliver given that the voltage and current are fixed when the SCXI-1163R was used. Thus, target levels of heat output were achieved by essentially switching the heaters on and off. The on-time or duty cycles for the heaters were varied based on the heat flux sensor readings. A LABVIEW subroutine was created for this feedback and control mechanism. The switching cycle of the subroutine was typically once every 3 seconds.

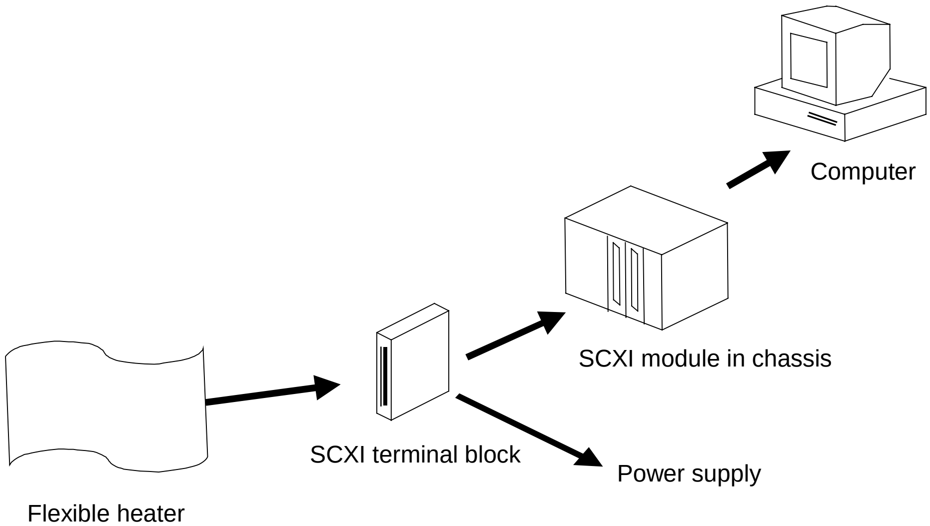

Figure 3.4: Schematic diagram of flexible heaters.

4 Experimental Results and Discussion

In this chapter, the measurements made in the steady-state flow-through experiments are described and the final values for relative permeability to steam and water are discussed.

4.1 General

A total of 22 steady-state experiments were conducted within a two-week period, excluding three runs for the wet scan. As noted in Section 2.3, the hot wet scan rather than the cold scan was the more appropriate measurement to make as far as obtaining steam saturation is concerned. Eleven runs were made each for the case of water displacement by steam (drainage) and steam displacement by water (imbibition). Near-adiabatic conditions were achieved in all but the first few low steam saturation runs of the drainage phase where the guard heater control system was not optimally configured. Maximum steam saturation of about 70% was reached.

Table 4.1 summarizes the important parameters relevant to the experiments conducted. The runs are labeled chronologically by steps. Steps 1 to 12 are for the drainage process while Steps 13 to 23 represent the imbibition stage.

Table 4.1: Summary of runs for the steady state experiments

	Steam			Water		
Step No.	Injection	Current	Voltage	Injection	Current	Voltage
1	10.00	1.100	65.0	10.00	0.768	45.0
3	4.50	0.845	50.0	4.00	0.678	40.0
4	4.50	0.845	50.0	3.50	0.678	40.0
5	4.00	0.845	50.0	3.00	0.678	40.0
6	4.00	1.092	65.0	2.75	0.577	35.0
7	2.25	1.176	70.0	3.75	0.577	35.0
8	3.50	1.173	70.0	1.50	0.577	35.0
9	3.50	1.344	80.0	0.75	0.674	40.0
10	3.70	1.556	94.4	0.25	0.457	30.0
11	3.90	1.650	100.2	0.10	0.462	30.0
12	3.90	1.640	100.0	0.10	0.457	30.0
13	3.70	1.627	99.6	2.30	0.465	30.0
14	3.60	1.609	98.5	0.40	0.375	24.8
15	3.50	1.605	98.2	0.50	0.340	23.4
16	3.00	1.514	92.6	1.00	0.382	25.3
17	3.00	1.433	87.6	2.00	0.385	25.4
18	3.00	1.437	88.0	2.50	0.470	30.6
19	2.50	1.240	75.2	3.00	0.471	30.5
20	1.50	0.992	60.0	3.50	0.527	34.0
21	0.50	0.538	32.5	4.50	0.646	40.5
22	1.00	0.580	35.1	4.00	0.644	40.4
23	2.50	0.369	24.1	2.50	0.423	25.5

4.2 Saturation

Spatial distributions of porosity and steam saturation were obtained from Equation 2.6 and 2.7, respectively, using CT values reported in Appendix A. Sample CT scans are shown in Figure 4.1a, and Figure 4.1b shows the porosity values along the core, from which an average of 24.7% was observed. Figure 4.2a and 4.2b show the saturation profiles for drainage and imbibition runs, respectively. Note that the drainage phase covered the saturation range rather well whereas the imbibition runs had higher steam saturation values. This failure to cover the saturation range during the cool-down stage was due to time constraints on the availability of the X-ray scanner. All runs show approximately constant saturation profiles with the exception of Step 3 which was far from adiabatic.

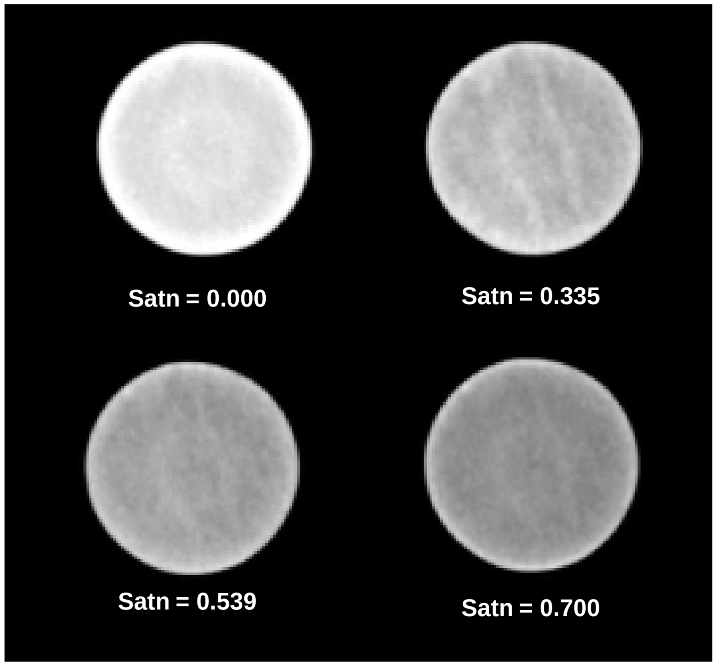

(a) Sample CT scans at x=16 cm from inlet.

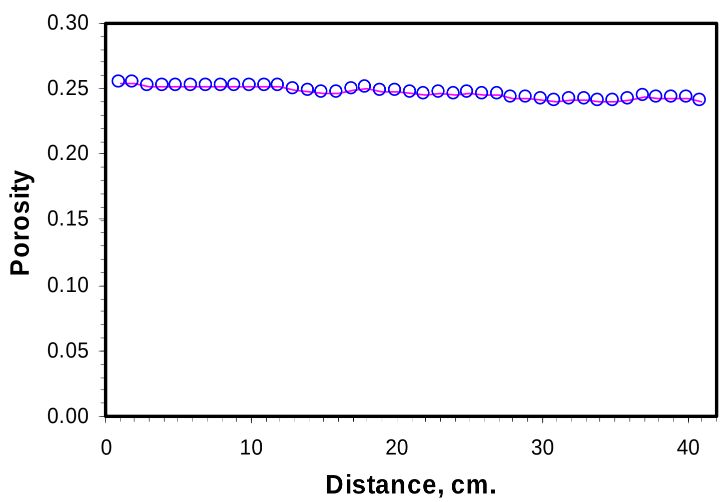

(b) Porosity distribution in the Berea core.

Figure 4.1: Results of X-ray CT scans.

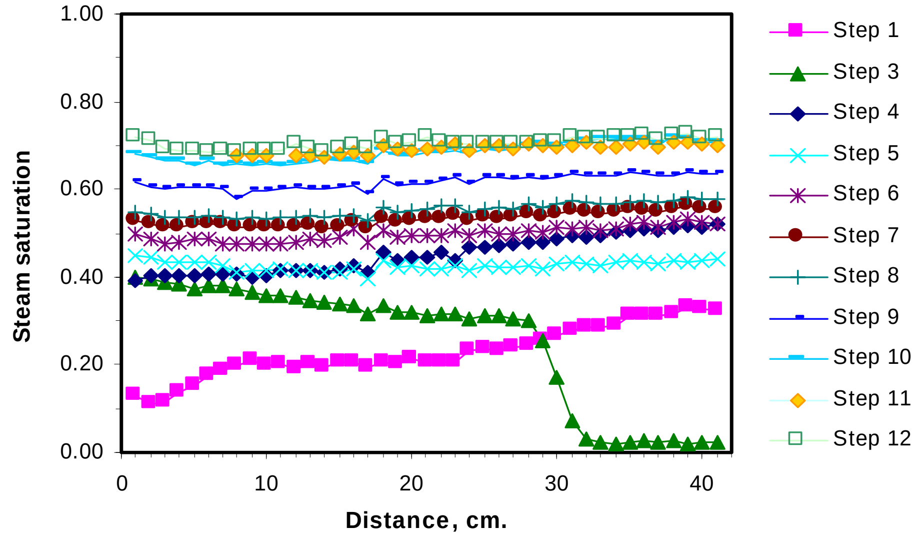

(a) Drainage

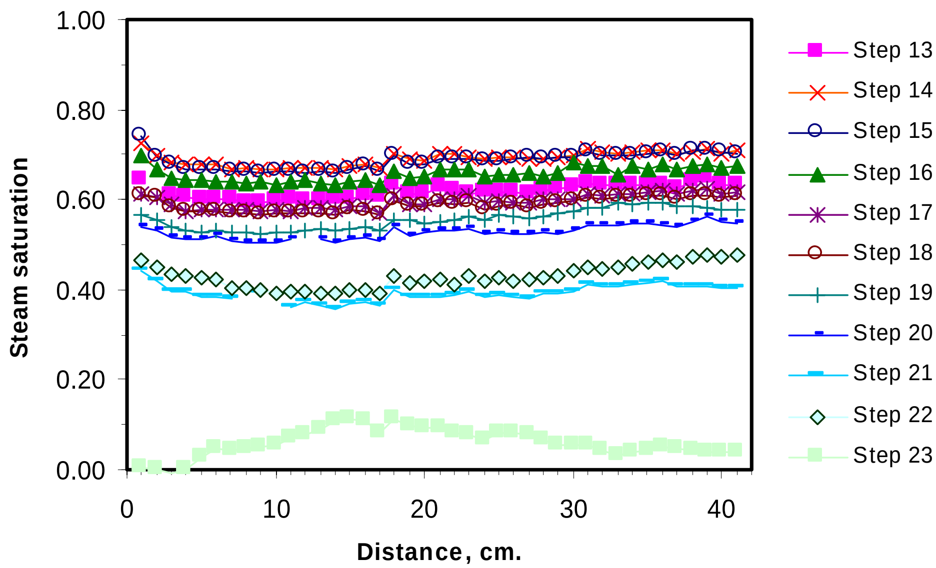

(b) Imbibition

Figure 4.2: Steam saturation profile for various steady state conditions.

4.3 Pressure

While it is ideal to conduct experiments with constant inlet pressure, this condition imposes a constraint that was difficult to achieve experimentally, especially with heat fluxes kept unchanged. Hence, we allowed inlet pressure to vary as necessary. Figures 4.3a and 4.3b are the pressure profiles for the drainage and imbibition cases, respectively. The maximum pressure reached was about 27 psig corresponding to the case of high average steam saturation within the core. The outlet pressure measurements did not vary since fluid exits the core at atmospheric conditions.

4.4 Temperature

The temperature profiles along the core are shown in Figures 4.4a and 4.4b. The maximum temperature achieved was 134 ^{O}C corresponding to the case of high steam saturation. These values do not match exactly, but are reasonably close to saturation temperatures at the measured pressures. The deviation is due to small instrument inaccuracy. The second thermocouple (at distance d=8.5 cm.) was not functioning properly during the drainage process, thus, measured temperature incorrectly.

4.5 Heat flux

Thermal losses were kept minimal with the aid of the flexible heaters and the associated control system. Figures 4.5a and 4.5b show heat fluxes measured from the core holder. Note that there were instances when average heat flux was negative. This implies a small amount of heating provided by the guard heaters. It is difficult to achieve a perfectly adiabatic experiment since the heaters were controlled by pulsing to achieve the desired level of output (see Section 3.4).

Similar relative permeability experiments conducted without the use of flexible heaters (Satik, 1998) reported heat fluxes ranging from 100 to 300 W/m^2. Heat fluxes were also observed to increase with increasing steam saturation. In contrast, the maximum absolute value of heat flux measured with the heat guard in use was approximately 100 W/m^2. Furthermore, heat loss does not necessarily increase with energy flux at the inlet because of the imposed adiabatic constraint. However, the flexible heaters had to have higher duty cycles (i.e., they had to be switched on more frequently) as a consequence.

4.6 Relative permeability curves

The analyses discussed in Chapter 2 applied to the experimental data gives the steam-water relative permeability values listed in Table 4.2. Figure 4.6 plots these data and differentiates between the drainage and imbibition phases of the experiments. Detailed calculation tables are given in Appendix B. Note that there are more data points than steady-state experiments since we were able to identify multiple flat-saturation regions within the core for a given step, thus, allowing more than one set of relative permeability values to be calculated. There are also fewer data points at higher liquid saturation (lower steam saturation) due to the issue of saturation coverage mentioned in Section 4.2. Several observations from the graphical results can be made.

As expected, relative permeability to water increased and that to steam decreased with liquid saturation. However, there appears to be more scatter in relative permeability to steam than to water. This may well be related to higher interstitial velocity and mobility of the steam phase that translates to a greater tendency to be more "chaotic" in its movement through the core.

From the graph, residual liquid saturation can be inferred to be around 30%. Residual steam saturation is, however, more challenging to estimate due to the sparseness of data at higher liquid saturations. Given this set of data, we may infer irreducible steam saturation for the given conditions to be between 10 and 20%.

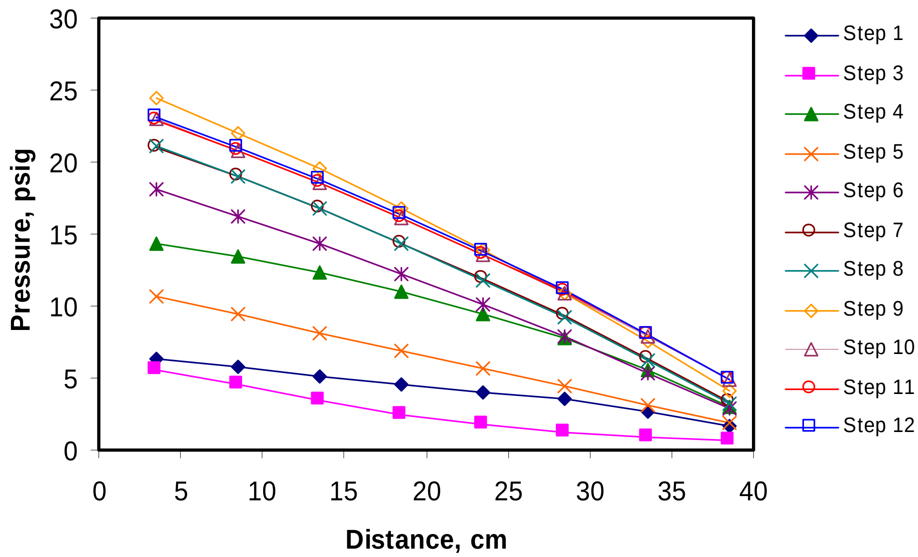

(a) Drainage

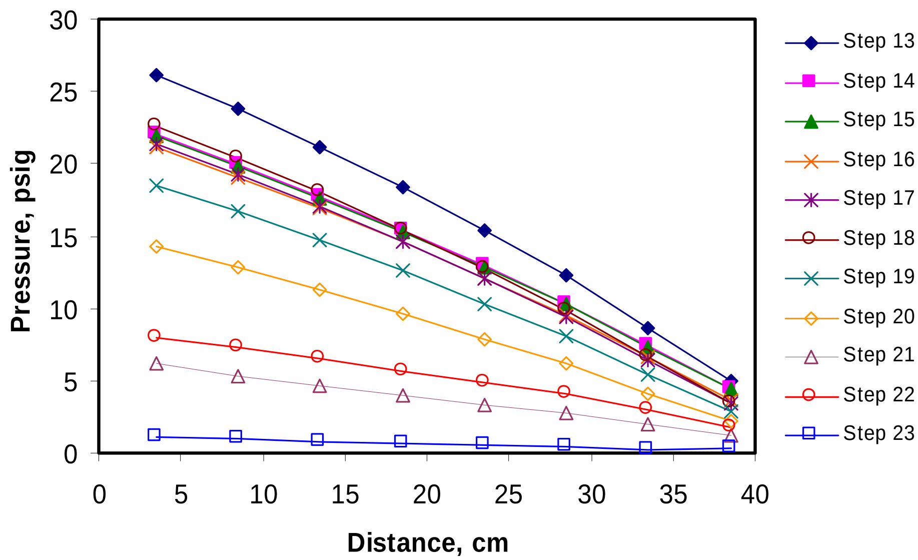

(b) Imbibition

Figure 4.3: Pressure profiles for steady experimental conditions.

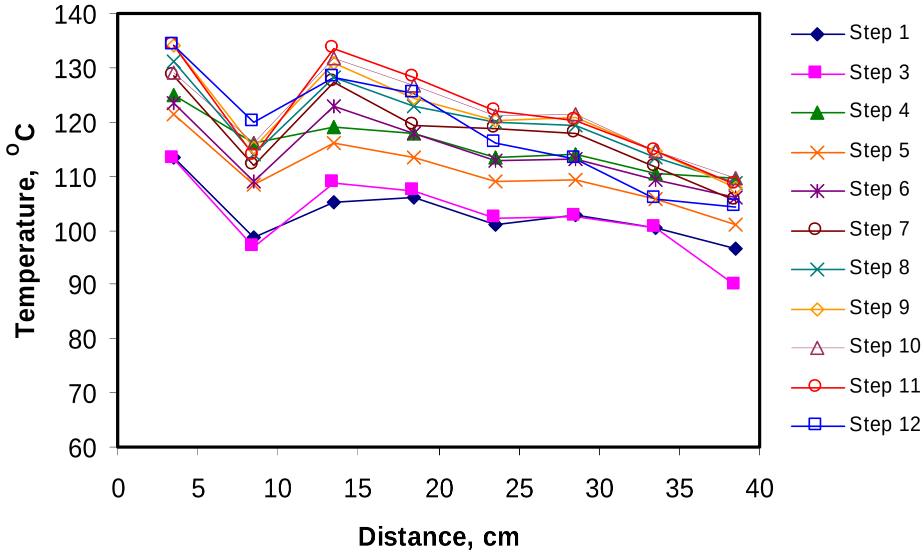

(a) Drainage

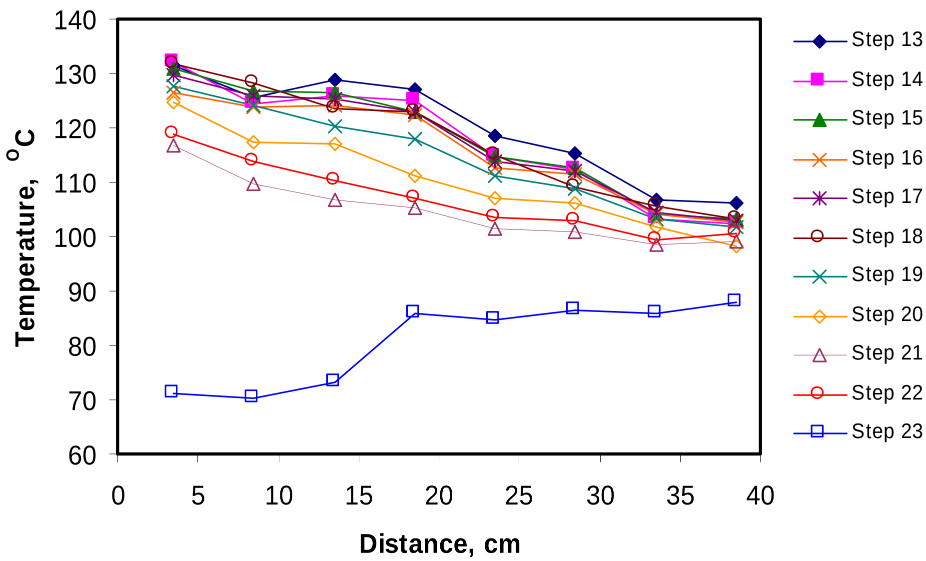

(b) Imbibition

Figure 4.4: Temperature profiles for steady experimental conditions.

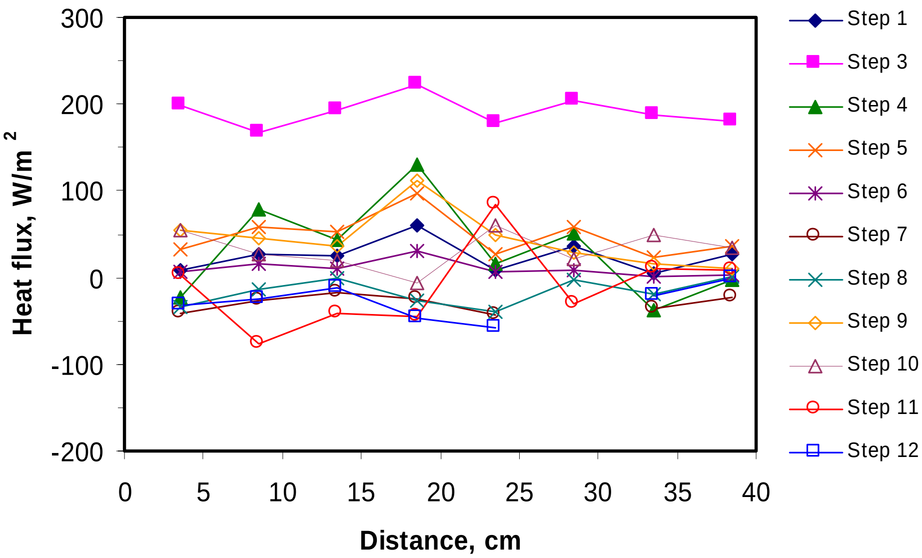

(a) Drainage

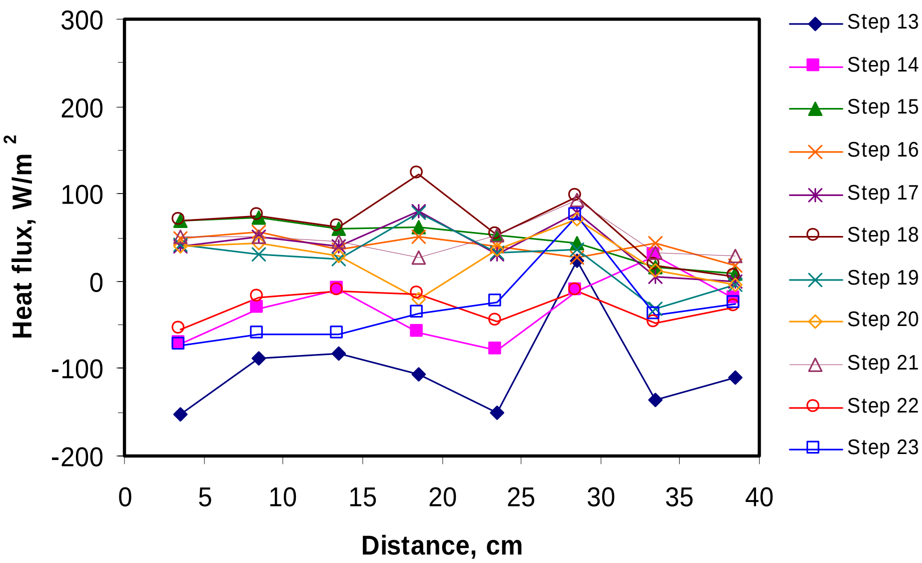

(b) Imbibition

Figure 4.5: Heat flux distribution for steady experimental conditions.

Table 4.3: Results of relative permeability experiments.

Drainage			Imbibition		
Sw	K_{rs}	K_{rw}	Sw	K_{rs}	K_{rw}
0.288	1.078	0.000	0.300	1.080	0.001
0.291	0.900	0.003	0.306	0.932	0.004
0.302	1.044	0.000	0.327	0.740	0.005
0.309	0.961	0.000	0.328	0.922	0.002
0.315	0.840	0.003	0.336	0.850	0.004
0.323	0.965	0.000	0.342	0.779	0.006
0.340	0.779	0.003	0.361	0.755	0.006
0.375	0.532	0.009	0.377	0.916	0.008
0.400	0.474	0.010	0.395	0.638	0.012
0.438	0.536	0.016	0.402	0.760	0.010
0.460	0.600	0.020	0.403	0.725	0.012
0.463	0.431	0.019	0.412	0.606	0.019
0.484	0.489	0.024	0.413	0.651	0.013
0.489	0.158	0.043	0.421	0.700	0.013
0.501	0.417	0.034	0.421	0.700	0.010
0.520	0.376	0.038	0.429	0.633	0.015
0.526	0.130	0.059	0.444	0.621	0.021
0.555	0.140	0.066	0.468	0.576	0.029
0.568	0.252	0.068	0.470	0.598	0.023
0.572	0.311	0.077	0.491	0.507	0.032
0.587	0.240	0.069	0.544	0.434	0.056
0.593	0.180	0.080	0.578	0.514	0.077
0.621	0.189	0.113	0.603	0.418	0.083
0.682	0.116	0.274	0.613	0.185	0.111
0.689	0.000	0.190	0.634	0.140	0.089
0.715	0.087	0.319	0.634	0.269	0.108
0.764	0.059	0.425	0.916	0.000	0.708
0.799	0.025	0.489	0.951	0.000	0.673
0.978	0.000	0.744			

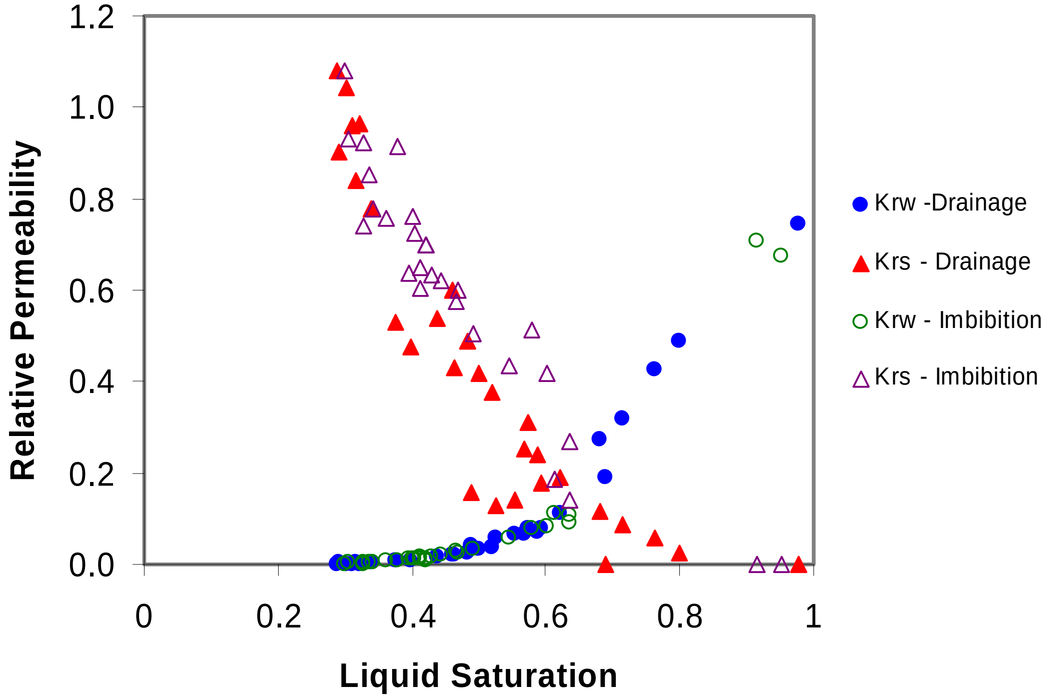

Figure 4.6: Plot of (uncorrected) steam-water relative permeability

A most interesting feature of these results is the existence of k_{rs} values greater than 1.0. This phenomenon was also observed in experiments conducted by Satik in 1998. Such seemingly erroneous values of relative permeability can be explained by considering the slip effect in single phase gas flow. Permeability of a porous medium measured by flowing single phase gas varies with the average pressure in the medium due to the Klinkenberg effect. A similar behavior may occur in combined vapor and liquid flow so a correction is necessary. From single-phase gas flow, the relative permeability, $k_{rg,corr}$, standardized to infinite pressure is given by

$$k_{rg,corr} = \frac{k_{rg}}{\left(1 + {b}/{p_m}\right)} \tag{4.1}$$

where k_{rg} is the relative permeability obtained at the measured average pressure, p_m. Assuming a slip factor, *b*, of 6.58 psia obtained from preliminary experiments by Li and Horne (1999), the "no-slip" relative permeability curves are as shown in Figure 4.7. Appendix C tabulates the data points for these curves.

Figure 4.8 compares the results of the current study to relative permeability curves from previous experimental works. The latest set of results is in closer agreement with the Corey-type curves obtained by Satik (1998) than with the linear-type curves obtained by Ambusso (1996). Relative to Satik (1998), the current k_{rs} values are generally higher and the intersection between the steam and liquid water curves are shifted from about 55% to 65% liquid saturation relative to Satik (1998). The curves for water, however, are nearly identical.

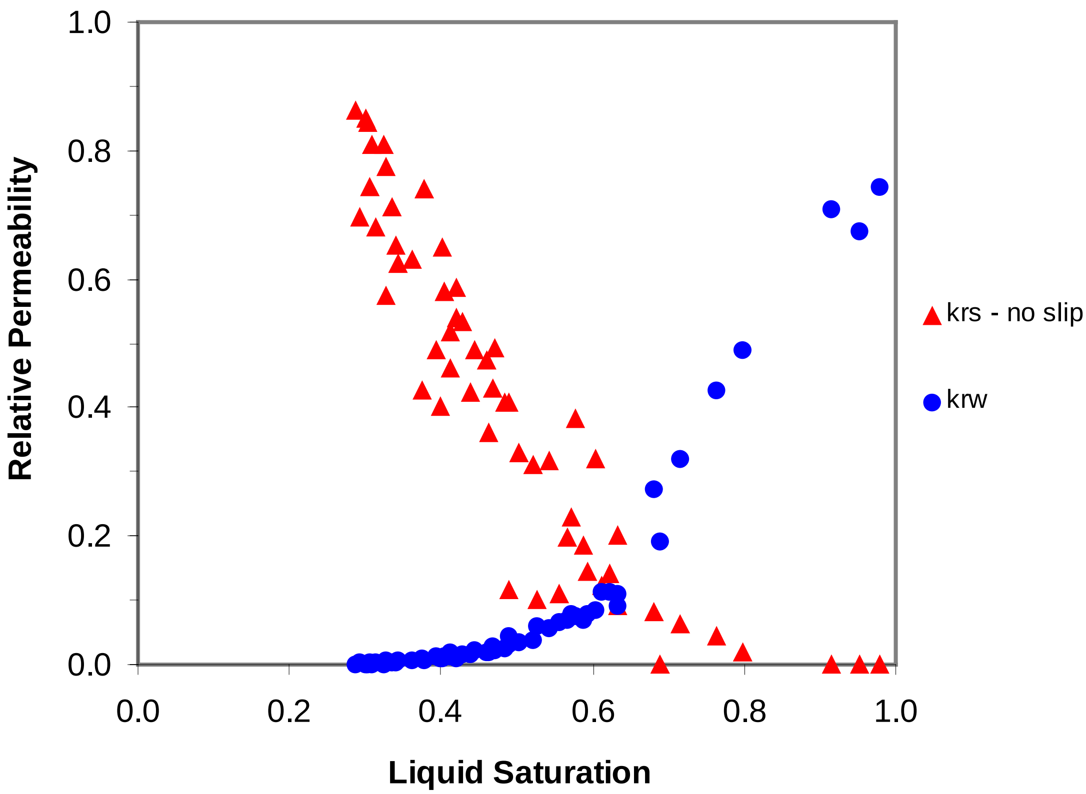

Figure 4.7 Relative permeability curves corrected for slip effect

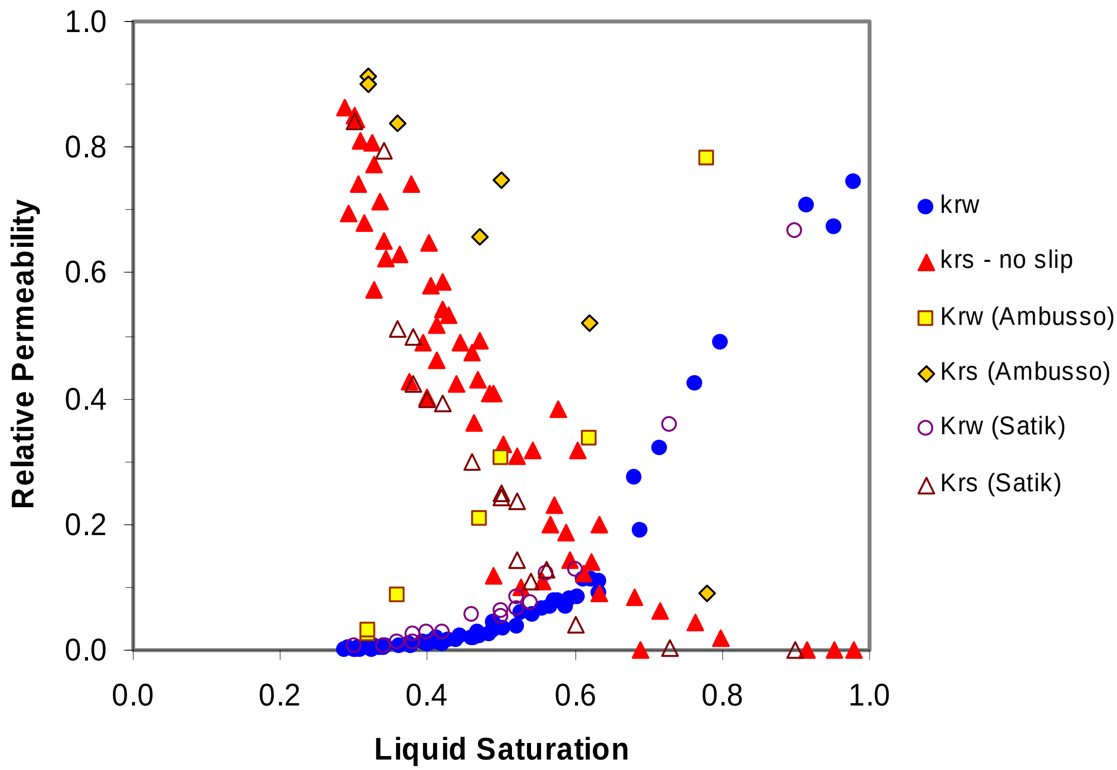

Figure 4.8: Comparison of obtained relative permeability curves

5 Conclusion

In this study, we have designed, implemented and interpreted results from steady-state flow-through experiments to obtain steam-water relative permeability relations. This project utilized measurements of pressure, temperature and heat fluxes in conjunction with in-situ steam saturation measurements from X-ray CT scans to establish the desired curves. With the aid of flexible heaters around the core holder and an accompanying feedback and control system, heat losses from the core were decreased to near-adiabatic conditions. This had the benefit of minimizing errors associated with heat flux measurements.

The set of relative permeability curves established from this study gives credence to a Corey-type profile. The curves are consistent with many previous experimental studies that found relative permeability to steam having a more pronounced effect than that to water, as evidenced by greater values assumed by the former (Verma, 1986; Clossman and Vinegar, 1988; Ambusso, 1996). Residual water saturation for the specific Berea sandstone used was found to be in the vicinity of 30%, whereas the residual steam saturation was between 10 and 20%. Slip effect in the flow of the vapor phase appears to be an important factor.

The behavior of steam and water flow in a porous medium depends on the thermodynamic and fluid properties as well as the petrophysical properties of the medium. It is, thus, reasonable to assume that relative permeability will vary with the average pressure under which fluid flows, and with the detailed structure of the porous medium that translates to bulk properties such as porosity and absolute permeability. Although this study focused on one type of rock with a specific set of properties and may be construed as rather limited in its application, it is still invaluable since: (1) it establishes a methodology that yields reproducible results, and (2) it gives an idea of the general shape of steam-water relative permeability curves. The set of results also lends itself as a baseline for future sensitivity studies that may be conducted employing the same experimental approach.

References

Ambusso, W.J., "Experimental Determination of Steam-Water Relative Permeability Relations," Masters thesis, Stanford University, Stanford, California (1996).

Ambusso, W.J., Satik, C., and Horne, R.N., "A Study of Relative Permeability for Steam-Water Flow in Porous Media," Proceedings of 21st Workshop on Geothermal Reservoir Engineering, Stanford University, Stanford, California (1996).

Arihara, N.: "A Study of Non-Isothermal Single and Two-Phase Flow Through Consolidated Sandstones," PhD dissertation, Stanford University, Stanford, California (1976).

Chen, J.K., Council, J.R., and Ramey, H.J., Jr., "Experimental Steam-Water Permeability Curves," GRC Trans. Vol. 2 (1978), pp 102-104.

Clossman, P.J. and Vinegar, J.J., "Relative Permeability to Steam and Water at Residual Oil in Natural Cores; CT Scan Saturation," SPE paper 174449.

Corey, A.T., "The Interrelations Between Gas and Oil Relative Permeabilities," Producers Monthly Vol. 19 (1954), pp 38-41.

Council, J.R. and Ramey Jr., H.J., "Drainage Relative Permeabilities Obtained from Steam-Water boiling Flow and External Gas Drive Experiments," GRC Trans. Vol 3 (1979), pp 141-143.

Grant, M.A., “Permeability Reduction Factors at Wairakei,” paper presented at AIChE-ASME Heat Transfer Conference, AIChE, Salt Lake City, Utah (August 1977), pp 15-17.

Horne R.N. and Ramey Jr. H.J., “Steam/Water Relative Permeability from Production Data,” GRC Trans. Vol. 2 (1978).

Li, K. and Horne, R.N., “Accurate Measurement of Steam Flow Properties,” paper to be published in GRC Trans. Vol. 23 (1999).

Piquemal, J., “Saturated Steam Relative Permeabilities of Unconsolidated Porous Media,” Transport in Porous Media 17 (1994), pp 105-120.

Sanchez, J.M. and Schechter, R.S., “Comparison of Two-phase Flow of Steam/Water through an Unconsolidated Permeable Medium, SPE paper 16967.

Satik, C., “A Measurement of Steam-Water Relative Permeability,” Proceedings of 23rd Workshop on Geothermal Reservoir Engineering, Stanford University, Stanford, Califonia (1998).

Sorey, M.L., Grant, M.A., and Bradford, E., “Nonlinear Effects in Two-phase Flow to Wells in Geothermal Reservoirs,” Water Resources Research, Vol. 16 No. 5 (1980), pp 767-777.

Verma, M.A., “Effects of Phase Transformation of Steam-Water Two-phase Relative Permeability,” PhD Thesis, University of California, Berkeley (1986).

Appendices

Appendix A : CT Values

Slice	Dry	Wet	Wet 2	Hot Water	Step 1	Step 3	Step 4	Step 5	Step 6
	1740	**1741-42**	**1743**	**1744**	**1746**	**1748**	**1749**	**1750**	**1751**
1	1007	1261	1261	1246	1215	1151	1152	1139	1127
2	1003	1257	1257	1241	1215	1147	1145	1135	1125
3	1004	1256	1256	1239	1212	1148	1144	1137	1127
4	1008	1260	1260	1243	1211	1153	1148	1141	1130
5	1007	1259	1259	1242	1206	1154	1147	1140	1128
6	1009	1261	1261	1244	1203	1155	1148	1142	1130
7	1008	1260	1260	1243	1199	1154	1147	1143	1131
8	1007	1259	1258	1241	1195	1154	1146	1145	1130
9	1011	1263	1263	1246	1197	1160	1152	1149	1134
10	1011	1262	1262	1245	1199	1161	1151	1148	1134
11	1013	1264	1264	1248	1201	1164	1151	1150	1136
12	1012	1263	1264	1247	1202	1164	1150	1150	1134
13	1012	1261	1261	1246	1199	1165	1149	1149	1132
14	1002	1252	1250	1234	1189	1155	1139	1139	1122
15	1005	1253	1252	1236	1189	1158	1139	1141	1123
16	1010	1257	1256	1240	1193	1163	1142	1144	1123
17	1019	1268	1268	1250	1205	1177	1155	1159	1139
18	1019	1269	1269	1253	1205	1175	1146	1151	1135
19	1025	1274	1273	1258	1211	1184	1156	1160	1144
20	1027	1275	1275	1259	1210	1185	1156	1160	1144
21	1032	1278	1278	1262	1215	1190	1160	1166	1148
22	1033	1277	1278	1261	1214	1189	1157	1166	1148
23	1029	1275	1276	1259	1212	1186	1158	1161	1143
24	1031	1274	1276	1260	1207	1190	1153	1165	1147
25	1031	1276	1277	1261	1207	1189	1153	1163	1145
26	1031	1276	1276	1260	1207	1189	1152	1163	1146
27	1035	1280	1280	1263	1208	1194	1155	1167	1149
28	1035	1278	1277	1262	1207	1194	1153	1165	1147
29	1035	1271	1277	1260	1203	1203	1152	1166	1147
30	1038	1279	1279	1264	1204	1225	1154	1167	1148
31	1039	1280	1279	1266	1203	1250	1154	1168	1150
32	1039	1282	1280	1267	1202	1260	1155	1169	1150
33	1036	1279	1277	1263	1198	1258	1151	1166	1148
34	1037	1280	1277	1264	1198	1260	1150	1166	1148
35	1036	1280	1276	1265	1194	1260	1149	1165	1146
36	1035	1279	1276	1265	1193	1259	1148	1165	1144
37	1033	1279	1277	1265	1193	1260	1148	1165	1146
38	1033	1277	1276	1264	1191	1258	1145	1163	1143
39	1038	1282	1280	1266	1191	1262	1148	1167	1145
40	1038	1281	1280	1268	1193	1263	1150	1167	1147
41	1040	1283	1280	1269	1195	1264	1150	1168	1150

Slice	Step 7 1752	Step 8 1753	Step 9 1755	Step 10 1756	Step 11 1757	Step 12 1758	Step 13 1759	Step 14 1760	Step 15 1761
1	1120	1115	1099	1083		1074	1092	1073	1069
2	1117	1112	1097	1081		1072		1075	1076
3	1118	1113	1098	1083		1076	1096	1079	1080
4	1122	1117	1101	1087		1081	1101	1084	1086
5	1120	1116	1100	1088		1080	1101	1083	1085
6	1122	1117	1102	1088		1083	1103	1085	1087
7	1121	1117	1102	1089		1081	1102	1086	1087
8	1121	1116	1106	1087	1083	1081	1102	1084	1086
9	1125	1120	1106	1092	1087	1084	1107	1089	1091
10	1125	1120	1105	1091	1087	1084	1105	1089	1090
11	1127	1122	1107	1094		1086	1107	1090	1092
12	1126	1121	1105	1092	1088	1082	1107	1089	1092
13	1125	1120	1105	1091	1088	1084	1106	1089	1091
14	1116	1110	1095	1079	1078	1075	1095	1079	1081
15	1117	1111	1096	1082	1079	1076	1097	1080	1082
16	1119	1116	1100	1087	1083	1079	1100	1084	1085
17	1132	1128	1114	1098	1094	1090	1110	1095	1097
18	1128	1122	1107	1092	1089	1086	1105	1089	1090
19	1136	1130	1116	1100	1097	1094	1115	1097	1100
20	1136	1131	1117	1102	1099	1095	1117	1100	1102
21	1140	1134	1121	1105	1103	1097	1118	1101	1103
22	1140	1133	1120	1105	1102	1100	1120	1101	1104
23	1135	1130	1115	1101	1097	1097	1118	1099	1100
24	1139	1135	1120	1104	1102	1099	1119	1102	1103
25	1138	1133	1117	1102	1100	1099	1119	1101	1103
26	1138	1132	1116	1102	1100	1099	1119	1101	1102
27	1141	1136	1121	1105	1105	1103	1123	1106	1105
28	1139	1133	1120	1103	1102	1102	1121	1105	1105
29	1139	1134	1120	1102	1103	1101	1120	1104	1104
30	1141	1136	1122	1106	1107	1104	1122	1106	1107
31	1141	1136	1122	1106	1107	1103	1122	1104	1106
32	1142	1137	1123	1105	1106	1104	1123	1106	1108
33	1140	1134	1120	1101	1105	1101	1120	1104	1105
34	1140	1135	1121	1102	1106	1101	1121	1104	1106
35	1138	1134	1119	1101	1104	1100	1120	1103	1104
36	1138	1133	1119	1101	1102	1099	1120	1102	1103
37	1138	1133	1119	1102	1104	1100	1120	1102	1103
38	1136	1131	1118	1098	1101	1097	1116	1101	1100
39	1138	1133	1120	1103	1105	1100	1118	1103	1104
40	1140	1135	1122	1105	1106	1104	1123	1107	1106
41	1142	1137	1124	1107	1109	1104	1124	1107	1108

Slice	Step 16 1762	Step 17 1763	Step 18 1764	Step 19 1765	Step 20 1768	Step 21 1769	Step 22 1770	Step 23 1771
1	1079	1100	1101	1111	1117	1140	1135	1245
2	1082	1097	1097	1109	1115	1141	1134	1241
3	1087	1101	1102	1112	1118	1146	1137	1241
4	1092	1108	1108	1118	1123	1150	1142	1243
5	1091	1106	1107	1118	1122	1152	1142	1236
6	1094	1108	1109	1119	1122	1154	1145	1233
7	1093	1107	1109	1119	1124	1154	1148	1233
8	1092	1106	1108	1118	1123		1147	1230
9	1096	1111	1113	1123	1128	1154	1152	1234
10	1097	1110	1112	1122	1127		1153	1232
11	1098	1113	1114	1124	1128	1163	1155	1232
12	1096	1110	1113	1122		1160	1154	1229
13	1097	1110	1113	1121	1126	1161	1154	1225
14	1087	1100	1103	1111	1117	1151	1143	1209
15	1088	1101	1103	1112	1118	1151	1144	1210
16	1092	1105	1108	1116	1121	1154	1148	1215
17	1104	1118	1119	1127	1133	1166	1160	1231
18	1098	1111	1113	1123	1127	1160	1152	1227
19	1107	1121	1122	1129	1137	1169	1161	1235
20	1108	1122	1123	1132	1137	1170	1162	1237
21	1109	1124	1126	1135	1140	1174	1165	1241
22	1109	1124	1127	1135	1140	1173	1167	1242
23	1106	1119	1123	1130	1136	1168	1160	1241
24	1111	1124	1128	1133	1140	1172	1164	1245
25	1110	1124	1126	1131	1140	1172	1163	1242
26	1110	1124	1125	1131	1140	1172	1164	1241
27	1113	1128	1130	1136	1144	1176	1167	1245
28	1114	1126	1128	1134	1142	1173	1165	1247
29	1112	1125	1127	1132	1142	1172	1163	1248
30	1110	1128	1129	1134	1144	1175	1164	1252
31	1113	1127	1129	1134	1143	1173	1164	1254
32	1113	1128	1130	1134	1143	1174	1165	1257
33	1114	1124	1126	1128	1140	1171	1161	1256
34	1111	1125	1127	1130	1140	1171	1160	1255
35	1112	1124	1126	1129	1140	1170	1159	1255
36	1109	1122	1125	1129	1140	1169	1158	1253
37	1110	1123	1126	1129	1140	1171	1158	1254
38	1108	1121	1123	1129	1137	1170	1155	1254
39	1111	1124	1127	1133	1138	1173	1157	1257
40	1114	1127	1129	1135	1141	1175	1159	1259
41	1115	1128	1130	1137	1144	1177	1160	1260

Appendix B : Calculations

Step 1

Position	Flowrate (cc/min)	Flowrate (kg/s)	Current (A)	Voltage (V)	Elec. Input (kJ/kg)
Steam line	10	1.67E-04	1.1	65	429.00
Water line	10	1.67E-04	0.768	45	207.36

Position	Distance (cm)	P (psig)	P(abs) (psia)	T (^oC)	T_{sat} (^oC)	$h_s(P)$ (kJ/kg)	$h_w(P)$ (kJ/kg)	Q_{lost} (W/m^2)	Enthalpy (kJ/kg)
Steam inlet	0	6.63	21.33	109.77	110.32	2693	463		463
Water inlet	0	5.79	20.49	79.43	109.12	2691	458		333
Port 1	3.5	6.28	20.98	113.35	109.83	2692	461	8.19	397
Port 2	8.5	5.74	20.44	98.68	109.05	2691	457	27.41	395
Port 3	13.5	5.14	19.84	105.30	108.19	2689	454	25.07	393
Port 4	18.5	4.61	19.31	105.97	107.41	2688	450	60.49	389
Port 5	23.5	4.04	18.74	101.04	106.57	2687	447	7.81	388
Port 6	28.5	3.61	18.31	102.88	105.91	2686	444	35.33	386
Port 7	33.5	2.71	17.41	100.58	104.55	2683	438	4.33	385
Port 8	38.5	1.65	16.35	96.74	102.90	2681	431	26.60	383
Outlet	43.5	0.41	15.11	103.37	100.94	2677	423	7.81	383

Position	X	μ_s (cp)	ρ_s (kg/m^3)	μ_w (cp)	ρ_w (kg/m^3)	k_{rs}	k_{rw}	S_w	P_{ave} (psig)
Steam inlet	1.0000	0.0127	0.85	0.2533	950.26				
Water inlet	0.0000	0.0126	0.81	0.2563	951.18				
Port 1	0.0000	0.0126	0.83	0.2545	950.64				
Port 2	0.0006	0.0126	0.81	0.2564	951.24				
Port 3	0.0014	0.0126	0.79	0.2586	951.89				
Port 4	0.0009	0.0126	0.77	0.2607	952.49	0.0249	0.4888	0.7987	5.17
Port 5	0.0022	0.0125	0.75	0.2629	953.13				
Port 6	0.0023	0.0125	0.73	0.2647	953.63	0.0591	0.4250	0.7638	3.38
Port 7	0.0047	0.0124	0.70	0.2685	954.66	0.0871	0.3194	0.7151	3.16
Port 8	0.0069	0.0124	0.66	0.2734	955.91	0.1156	0.2739	0.6818	2.18
Outlet	0.0104	0.0123	0.61	0.2797	957.39				

Step 3

Position	Flowrate (cc/min)	Flowrate (kg/s)	Current (A)	Voltage (V)	Elec. Input (kJ/kg)
Steam line	4.5	7.50E-05	0.845	50	563.33
Water line	4	6.67E-05	0.678	40	406.80

Position	Distance (cm)	P (psig)	P(abs) (psia)	T (^oC)	Tsat (^oC)	$h_s(P)$ (kJ/kg)	$h_w(P)$ (kJ/kg)	Q_{lost} (W/m^2)	Enthalpy (kJ/kg)
Steam inlet	0	6.41	21.11	108.73	110.01	2692	461		730
Water inlet	0	5.62	20.32	95.18	108.89	2690	457		399
Port 1	3.5	5.56	20.26	113.08	108.79	2690	456	198.30	540
Port 2	8.5	4.52	19.22	97.04	107.28	2688	450	167.00	511
Port 3	13.5	3.44	18.14	108.74	105.66	2685	443	193.07	478
Port 4	18.5	2.50	17.20	107.32	104.22	2683	437	221.97	439
Port 5	23.5	1.77	16.47	102.20	103.10	2681	432	178.86	408
Port 6	28.5	1.17	15.87	102.56	102.15	2679	428	203.21	373
Port 7	33.5	0.86	15.56	100.36	101.66	2678	426	187.35	340
Port 8	38.5	0.69	15.39	89.74	101.39	2678	425	179.62	309
Outlet	43.5	0.20	14.90	93.82	100.59	2676	422	164.04	295

Position	X	μ_s (cp)	ρ_s (kg/m^3)	μ_w (cp)	ρ_w (kg/m^3)	k_{rs}	k_{rw}	S_w	P_{ave} (psig)
Steam inlet	1.0000	0.0126	0.84	0.2541	950.50				
Water inlet	0.0000	0.0126	0.81	0.2569	951.36				
Port 1	0.0375	0.0126	0.81	0.2571	951.44				
Port 2	0.0273	0.0126	0.77	0.2610	952.58	0.1888	0.1126	0.6213	5.04
Port 3	0.0154	0.0125	0.73	0.2654	953.82				
Port 4	0.0010	0.0124	0.69	0.2695	954.91				
Port 5	0.0000	0.0124	0.66	0.2728	955.76				
Port 6	0.0000	0.0124	0.64	0.2758	956.47	0.0000	0.1897	0.6886	1.83
Port 7	0.0000	0.0123	0.63	0.2773	956.85				
Port 8	0.0000	0.0123	0.62	0.2782	957.05	0.0000	0.7444	0.9782	0.78
Outlet	0.0000	0.0123	0.61	0.2808	957.65				

Step 4

Position	Flowrate (cc/min)	Flowrate (kg/s)	Current (A)	Voltage (V)	Elec. Input (kJ/kg)
Steam line	4.5	7.50E-05	0.845	50	563.33
Water line	3.5	5.83E-05	0.678	40	464.91

Position	Distance (cm)	P (psig)	P(abs) (psia)	T (^oC)	T_{sat} (^oC)	$h_s(P)$ (kJ/kg)	$h_w(P)$ (kJ/kg)	Q_{lost} (W/m^2)	Enthalpy (kJ/kg)
Steam inlet	0	14.78	29.48	121.28	120.78	2707	507		730
Water inlet	0	14.01	28.71	108.81	119.87	2706	503		456
Port 1	3.5	14.32	29.02	124.80	120.24	2706	505	-22.89	615
Port 2	8.5	13.47	28.17	116.01	119.24	2705	500	78.44	600
Port 3	13.5	12.37	27.07	119.02	117.90	2703	495	42.98	592
Port 4	18.5	11.02	25.72	117.75	116.21	2701	488	129.62	568
Port 5	23.5	9.49	24.19	113.37	114.22	2698	479	16.40	565
Port 6	28.5	7.72	22.42	114.09	111.85	2695	469	50.74	556
Port 7	33.5	5.51	20.21	110.46	108.73	2690	456	-38.47	563
Port 8	38.5	3.01	17.71	109.49	105.02	2684	440	-3.41	564
Outlet	43.5	0.21	14.91	98.73	100.62	2677	422	-0.81	564

Position	X	μ_s (cp)	ρ_s (kg/m^3)	μ_w (cp)	ρ_w (kg/m^3)	k_{rs}	k_{rw}	S_w	P_{ave} (psig)
Steam inlet	1.0000	0.0130	1.15	0.2308	942.15				
Water inlet	0.0000	0.0130	1.12	0.2326	942.86				
Port 1	0.0500	0.0130	1.13	0.2319	942.57				
Port 2	0.0453	0.0130	1.10	0.2338	943.36				
Port 3	0.0442	0.0129	1.06	0.2365	944.40	0.1799	0.0798	0.5930	12.25
Port 4	0.0365	0.0129	1.01	0.2401	945.72				
Port 5	0.0389	0.0128	0.95	0.2443	947.26	0.1398	0.0663	0.5547	10.25
Port 6	0.0391	0.0127	0.89	0.2497	949.09	0.1302	0.0588	0.5263	8.60
Port 7	0.0480	0.0126	0.80	0.2573	951.48				
Port 8	0.0551	0.0125	0.71	0.2672	954.31	0.1582	0.0434	0.4891	4.26
Outlet	0.0631	0.0123	0.61	0.2807	957.63				

Step 5

Position	Flowrate (cc/min)	(kg/s)	Current (A)	Voltage (V)	Elec. Input (kJ/kg)
Steam line	4	6.67E-05	0.845	50	633.75
Water line	3	5.00E-05	0.678	40	542.40

Position	Distance (cm)	P (psig)	P(abs) (psia)	T (^oC)	T_{sat} (^oC)	$h_s(P)$ (kJ/kg)	$h_w(P)$ (kJ/kg)	Q_{lost} (W/m^2)	Enthalpy (kJ/kg)
Steam inlet	0	11.60	26.30	115.52	116.94	2702	491		801
Water inlet	0	10.76	25.46	104.43	115.88	2701	486		438
Port 1	3.5	10.71	25.41	121.34	115.82	2700	486	32.01	638
Port 2	8.5	9.44	24.14	108.35	114.17	2698	479	58.61	626
Port 3	13.5	8.14	22.84	116.11	112.41	2696	472	53.60	615
Port 4	18.5	6.85	21.55	113.35	110.63	2693	464	96.39	595
Port 5	23.5	5.61	20.31	109.06	108.87	2690	457	26.80	589
Port 6	28.5	4.41	19.11	109.22	107.11	2688	449	58.95	576
Port 7	33.5	3.06	17.76	105.84	105.09	2684	441	22.82	572
Port 8	38.5	1.83	16.53	101.00	103.19	2681	433	35.87	564
Outlet	43.5	0.42	15.12	96.57	100.95	2677	423	28.48	561

Position	X	μ_s (cp)	ρ_s (kg/m^3)	μ_w (cp)	ρ_w (kg/m^3)	k_{rs}	k_{rw}	S_w	P_{ave} (psig)
Steam inlet	1.0000	0.0129	1.03	0.2385	945.15				
Water inlet	0.0000	0.0128	1.00	0.2408	945.98				
Port 1	0.0689	0.0128	1.00	0.2409	946.02				
Port 2	0.0663	0.0128	0.95	0.2445	947.30	0.2520	0.0680	0.5677	10.08
Port 3	0.0644	0.0127	0.90	0.2484	948.66				
Port 4	0.0586	0.0127	0.85	0.2526	950.03	0.2400	0.0691	0.5867	8.15
Port 5	0.0593	0.0126	0.81	0.2569	951.37				
Port 6	0.0569	0.0125	0.76	0.2614	952.71				
Port 7	0.0585	0.0125	0.71	0.2670	954.25				
Port 8	0.0585	0.0124	0.67	0.2725	955.69	0.3111	0.0768	0.5723	4.34
Outlet	0.0613	0.0123	0.61	0.2796	957.38				

Step 6

Position	Flowrate (cc/min)	Flowrate (kg/s)	Current (A)	Voltage (V)	Elec. Input (kJ/kg)
Steam line	4	6.67E-05	1.092	65	1064.70
Water line	2.75	4.58E-05	0.577	35	440.62

Position	Distance (cm)	P (psig)	P(abs) (psia)	T (^oC)	T_{sat} (^oC)	$h_s(P)$ (kJ/kg)	$h_w(P)$ (kJ/kg)	Q_{lost} (W/m^2)	Enthalpy (kJ/kg)
Steam inlet	0	19.28	33.98	120.29	125.64	2714	528		1232
Water inlet	0	18.12	32.82	98.98	124.45	2712	523		415
Port 1	3.5	18.06	32.76	123.57	124.38	2712	522	7.07	897
Port 2	8.5	16.24	30.94	108.99	122.42	2709	514	16.34	894
Port 3	13.5	14.35	29.05	122.92	120.27	2706	505	10.63	891
Port 4	18.5	12.27	26.97	117.88	117.78	2703	494	30.39	885
Port 5	23.5	10.11	24.81	112.86	115.04	2699	483	6.90	883
Port 6	28.5	7.90	22.60	113.27	112.09	2695	470	7.57	882
Port 7	33.5	5.37	20.07	109.17	108.53	2690	455	1.28	881
Port 8	38.5	2.86	17.56	106.03	104.78	2684	439	2.13	881
Outlet	43.5	0.21	14.91	101.24	100.62	2677	422	1.08	881

Position	X	μ_s (cp)	ρ_s (kg/m^3)	μ_w (cp)	ρ_w (kg/m^3)	k_{rs}	k_{rw}	S_w	P_{ave} (psig)
Steam inlet	1.0000	0.0132	1.31	0.2216	938.28				
Water inlet	0.0000	0.0131	1.27	0.2238	939.23				
Port 1	0.1713	0.0131	1.26	0.2239	939.28				
Port 2	0.1730	0.0131	1.20	0.2276	940.85				
Port 3	0.1756	0.0130	1.13	0.2318	942.55	0.3762	0.0378	0.5203	16.20
Port 4	0.1768	0.0129	1.05	0.2368	944.50				
Port 5	0.1808	0.0128	0.97	0.2425	946.63				
Port 6	0.1850	0.0127	0.89	0.2491	948.90	0.4170	0.0339	0.5014	10.09
Port 7	0.1908	0.0126	0.80	0.2578	951.64				
Port 8	0.1968	0.0125	0.71	0.2679	954.49				
Outlet	0.2036	0.0123	0.61	0.2807	957.63				

Step 7

Position	Flowrate (cc/min)	Flowrate (kg/s)	Current (A)	Voltage (V)	Elec. Input (kJ/kg)
Steam line	2.25	3.75E-05	1.176	70	2195.20
Water line	3.75	6.25E-05	0.577	35	323.12

Position	Distance (cm)	P (psig)	P(abs) (psia)	T (^oC)	T_{sat} (^oC)	$h_s(P)$ (kJ/kg)	$h_w(P)$ (kJ/kg)	Q_{lost} (W/m^2)	Enthalpy (kJ/kg)
Steam inlet	0	22.35	37.05	125.99	128.60	2717	540		2362
Water inlet	0	21.22	35.92	114.80	127.55	2716	536		482
Port 1	3.5	21.02	35.72	128.63	127.35	2716	535	-41.71	1197
Port 2	8.5	18.96	33.66	111.97	125.31	2713	526	-26.11	1204
Port 3	13.5	16.77	31.47	127.20	123.00	2710	516	-17.85	1208
Port 4	18.5	14.37	29.07	119.32	120.30	2707	505	-23.90	1214
Port 5	23.5	11.89	26.59	118.80	117.31	2703	492	-42.66	1224
Port 6	28.5	9.30	24.00	117.94	113.98	2698	478	0.00	1224
Port 7	33.5	6.31	21.01	111.66	109.88	2692	461	-35.51	1233
Port 8	38.5	3.33	18.03	105.53	105.50	2685	442	-23.52	1239
Outlet	43.5	0.27	14.97	98.81	100.71	2677	422	-16.20	1241

Position	X	μ_s (cp)	ρ_s (kg/m^3)	μ_w (cp)	ρ_w (kg/m^3)	k_{rs}	k_{rw}	S_w	P_{ave} (psig)
Steam inlet	1.0000	0.0133	1.42	0.2161	935.87				
Water inlet	0.0000	0.0132	1.38	0.2181	936.73				
Port 1	0.3037	0.0132	1.37	0.2184	936.88				
Port 2	0.3097	0.0132	1.30	0.2222	938.54				
Port 3	0.3153	0.0131	1.22	0.2265	940.38	0.4894	0.0238	0.4841	18.90
Port 4	0.3220	0.0130	1.13	0.2317	942.52				
Port 5	0.3312	0.0129	1.04	0.2378	944.87				
Port 6	0.3361	0.0128	0.94	0.2449	947.45				
Port 7	0.3461	0.0126	0.83	0.2544	950.60	0.6001	0.0200	0.4598	10.34
Port 8	0.3551	0.0125	0.72	0.2658	953.94				
Outlet	0.3631	0.0123	0.61	0.2804	957.56				

Step 8

Position	Flowrate (cc/min)	Flowrate (kg/s)	Current (A)	Voltage (V)	Elec. Input (kJ/kg)
Steam line	3.5	5.83E-05	1.173	70	1407.60
Water line	1.5	2.50E-05	0.577	35	807.80

Position	Distance (cm)	P (psig)	P(abs) (psia)	T (^oC)	T_{sat} (^oC)	$h_s(P)$ (kJ/kg)	$h_w(P)$ (kJ/kg)	Q_{lost} (W/m^2)	Enthalpy (kJ/kg)
Steam inlet	0	22.54	37.24	127.18	128.76	2718	541		1575
Water inlet	0	21.40	36.10	117.32	127.71	2716	536		492
Port 1	3.5	21.11	35.81	131.25	127.44	2716	535	-34.67	1260
Port 2	8.5	18.99	33.69	113.94	125.35	2713	526	-13.83	1264
Port 3	13.5	16.76	31.46	129.16	123.00	2710	516	-1.50	1265
Port 4	18.5	14.33	29.03	122.77	120.25	2706	505	-26.79	1273
Port 5	23.5	11.83	26.53	120.02	117.24	2702	492	-39.10	1284
Port 6	28.5	9.22	23.92	119.23	113.87	2698	478	-2.45	1285
Port 7	33.5	6.23	20.93	113.54	109.75	2692	460	-19.55	1291
Port 8	38.5	3.26	17.96	108.68	105.39	2685	442	1.20	1290
Outlet	43.5	0.21	14.91	101.10	100.61	2677	422	2.14	1290

Position	X	μ_s (cp)	ρ_s (kg/m^3)	μ_w (cp)	ρ_w (kg/m^3)	k_{rs}	k_{rw}	S_w	P_{ave} (psig)
Steam inlet	1.0000	0.0133	1.43	0.2158	935.73				
Water inlet	0.0000	0.0132	1.39	0.2178	936.59				
Port 1	0.3324	0.0132	1.37	0.2183	936.81				
Port 2	0.3374	0.0132	1.30	0.2221	938.51				
Port 3	0.3411	0.0131	1.22	0.2265	940.39	0.4314	0.0187	0.4634	18.94
Port 4	0.3488	0.0130	1.13	0.2318	942.56				
Port 5	0.3584	0.0129	1.04	0.2379	944.92				
Port 6	0.3636	0.0128	0.94	0.2451	947.53				
Port 7	0.3721	0.0126	0.83	0.2547	950.70	0.5364	0.0159	0.4378	10.28
Port 8	0.3782	0.0125	0.72	0.2661	954.02				
Outlet	0.3851	0.0123	0.61	0.2808	957.64				

Step 9

Position	Flowrate (cc/min)	Flowrate (kg/s)	Current (A)	Voltage (V)	Elec. Input (kJ/kg)
Steam line	3.5	5.83E-05	1.344	80	1843.20
Water line	0.75	1.25E-05	0.674	40	2156.80

Position	Distance (cm)	P (psig)	P(abs) (psia)	T (^oC)	T_{sat} (^oC)	$h_s(P)$ (kJ/kg)	$h_w(P)$ (kJ/kg)	Q_{lost} (W/m^2)	Enthalpy (kJ/kg)
Steam inlet	0	26.05	40.75	128.50	131.76	2722	554		2010
Water inlet	0	24.94	39.64	117.64	130.85	2720	550		494
Port 1	3.5	24.43	39.13	134.21	130.43	2720	548	54.34	1724
Port 2	8.5	22.05	36.75	115.10	128.32	2717	539	44.61	1708
Port 3	13.5	19.53	34.23	130.74	125.89	2714	529	36.20	1696
Port 4	18.5	16.75	31.45	124.28	122.98	2710	516	110.97	1657
Port 5	23.5	13.93	28.63	120.13	119.78	2706	503	49.48	1640
Port 6	28.5	10.94	25.64	120.90	116.11	2701	487	28.74	1630
Port 7	33.5	7.52	22.22	114.55	111.57	2694	468	15.06	1625
Port 8	38.5	4.10	18.80	107.96	106.65	2687	447	10.42	1621
Outlet	43.5	0.58	15.28	100.94	101.21	2678	424	0.47	1621

Position	X	μ_s (cp)	ρ_s (kg/m^3)	μ_w (cp)	ρ_w (kg/m^3)	k_{rs}	k_{rw}	S_w	P_{ave} (psig)
Steam inlet	1.0000	0.0134	1.55	0.2103	933.23				
Water inlet	0.0000	0.0133	1.51	0.2120	934.00				
Port 1	0.5414	0.0133	1.49	0.2128	934.35				
Port 2	0.5369	0.0133	1.41	0.2167	936.09				
Port 3	0.5341	0.0132	1.32	0.2211	938.07	0.4743	0.0098	0.3997	21.98
Port 4	0.5201	0.0131	1.22	0.2266	940.40				
Port 5	0.5163	0.0130	1.11	0.2328	942.93				
Port 6	0.5163	0.0129	1.01	0.2403	945.80				
Port 7	0.5196	0.0127	0.88	0.2503	949.31	0.5317	0.0090	0.3748	12.13
Port 8	0.5242	0.0125	0.75	0.2627	953.07				
Outlet	0.5312	0.0123	0.62	0.2788	957.19				

Step 10

Position	Flowrate (cc/min)	(kg/s)	Current (A)	Voltage (V)	Elec. Input (kJ/kg)
Steam line	3.7	6.17E-05	1.556	94.4	2381.94
Water line	0.25	4.17E-06	0.457	30	3290.40

Position	Distance (cm)	P (psig)	P(abs) (psia)	T (^oC)	T_{sat} (^oC)	$h_s(P)$ (kJ/kg)	$h_w(P)$ (kJ/kg)	Q_{lost} (W/m^2)	Enthalpy (kJ/kg)
Steam inlet	0	24.35	39.05	130.06	130.36	2720	548		2549
Water inlet	0	23.26	37.96	118.72	129.41	2718	544		498
Port 1	3.5	22.97	37.67	129.03	129.15	2718	542	55.29	2399
Port 2	8.5	20.82	35.52	116.08	127.16	2716	534	27.43	2388
Port 3	13.5	18.56	33.26	131.63	124.91	2713	524	19.13	2381
Port 4	18.5	16.10	30.80	126.75	122.27	2709	513	-7.00	2384
Port 5	23.5	13.57	28.27	121.17	119.35	2705	501	59.74	2361
Port 6	28.5	10.90	25.60	121.30	116.06	2701	487	21.18	2354
Port 7	33.5	7.86	22.56	114.51	112.04	2695	470	49.40	2335
Port 8	38.5	4.84	19.54	109.57	107.75	2689	452	34.34	2322
Outlet	43.5	1.54	16.24	101.73	102.74	2680	431	27.33	2317

Position	X	μ_s (cp)	ρ_s (kg/m^3)	μ_w (cp)	ρ_w (kg/m^3)	k_{rs}	k_{rw}	S_w	P_{ave} (psig)
Steam inlet	1.0000	0.0133	1.49	0.2129	934.41				
Water inlet	0.0000	0.0133	1.45	0.2147	935.20				
Port 1	0.8531	0.0133	1.44	0.2151	935.41				
Port 2	0.8500	0.0132	1.36	0.2188	937.04				
Port 3	0.8485	0.0131	1.28	0.2230	938.86	0.7792	0.0032	0.3396	19.69
Port 4	0.8518	0.0131	1.19	0.2279	940.97				
Port 5	0.8440	0.0130	1.10	0.2336	943.27				
Port 6	0.8432	0.0129	1.00	0.2404	945.84	0.8402	0.0031	0.3151	13.50
Port 7	0.8382	0.0127	0.89	0.2493	948.94				
Port 8	0.8362	0.0126	0.78	0.2598	952.22	0.9004	0.0030	0.2914	7.87
Outlet	0.8386	0.0124	0.66	0.2739	956.03				

Step 11

Position	Flowrate (cc/min)	Flowrate (kg/s)	Current (A)	Voltage (V)	Elec. Input (kJ/kg)
Steam line	3.9	6.50E-05	1.65	100.2	2543.54
Water line	0.1	1.67E-06	0.462	30	8316.00

Position	Distance (cm)	P (psig)	P(abs) (psia)	T (^oC)	T_{sat} (^oC)	$h_s(P)$ (kJ/kg)	$h_w(P)$ (kJ/kg)	Q_{lost} (W/m^2)	Enthalpy (kJ/kg)
Steam inlet	0	24.26	38.96	136.63	130.28	2720	547		2720
Water inlet	0	23.02	37.72	154.01	129.20	2718	543		2718
Port 1	3.5	22.89	37.59	134.09	129.09	2718	542	3.50	2718
Port 2	8.5	20.78	35.48	113.79	127.12	2715	534	-76.31	2746
Port 3	13.5	18.56	33.26	133.65	124.90	2713	524	-40.70	2761
Port 4	18.5	16.11	30.81	128.25	122.28	2709	513	-44.45	2778
Port 5	23.5	13.61	28.31	121.99	119.40	2705	501	83.79	2747
Port 6	28.5	10.96	25.66	120.18	116.14	2701	487	-31.10	2758
Port 7	33.5	7.95	22.65	114.63	112.15	2695	470	9.94	2755
Port 8	38.5	4.93	19.63	108.54	107.87	2689	452	7.68	2752
Outlet	43.5	1.59	16.29	100.06	102.81	2680	431	3.50	2751

Position	X	μ_s (cp)	ρ_s (kg/m^3)	μ_w (cp)	ρ_w (kg/m^3)	k_{rs}	k_{rw}	S_w	P_{ave} (psig)
Steam inlet	1.0000	0.0133	1.49	0.2131	934.48				
Water inlet	0.0000	0.0133	1.44	0.2150	935.37				
Port 1	1.0001	0.0133	1.44	0.2153	935.46				
Port 2	1.0142	0.0132	1.36	0.2189	937.07				
Port 3	1.0223	0.0131	1.28	0.2230	938.87	0.9655	0.0000	0.3233	19.67
Port 4	1.0313	0.0131	1.19	0.2279	940.96				
Port 5	1.0189	0.0130	1.10	0.2335	943.23				
Port 6	1.0260	0.0129	1.01	0.2402	945.78	1.0436	0.0000	0.3019	13.54
Port 7	1.0267	0.0127	0.89	0.2490	948.86				
Port 8	1.0282	0.0126	0.78	0.2594	952.13				
Outlet	1.0315	0.0124	0.66	0.2737	955.98				

Step 12

Position	Flowrate (cc/min)	(kg/s)	Current (A)	Voltage (V)	Elec. Input (kJ/kg)
Steam line	3.9	6.50E-05	1.64	100	2523.08
Water line	0.1	1.67E-06	0.457	30	8226.00

Position	Distance (cm)	P (psig)	P(abs) (psia)	T (^oC)	T_{sat} (^oC)	$h_s(P)$ (kJ/kg)	$h_w(P)$ (kJ/kg)	Q_{lost} (W/m^2)	Enthalpy (kJ/kg)
Steam inlet	0	24.49	39.19	117.10	130.47	2720	548		2690
Water inlet	0	23.27	37.97	157.91	129.42	2719	544		2719
Port 1	3.5	23.12	37.82	134.00	129.29	2718	543	-31.76	2702
Port 2	8.5	21.01	35.71	119.81	127.34	2716	535	-24.47	2712
Port 3	13.5	18.77	33.47	128.11	125.12	2713	525	-11.24	2716
Port 4	18.5	16.31	31.01	125.23	122.50	2709	514	-47.14	2733
Port 5	23.5	13.77	28.47	116.13	119.59	2706	502	-58.51	2755
Port 6	28.5	11.08	25.78	113.13	116.29	2701	488	15.83	2749
Port 7	33.5	8.00	22.70	105.72	112.22	2695	471	-21.18	2757
Port 8	38.5	4.94	19.64	104.15	107.89	2689	452	-0.31	2757
Outlet	43.5	1.55	16.25	97.91	102.74	2680	431	-11.44	2759

Position	X	μ_s (cp)	ρ_s (kg/m^3)	μ_w (cp)	ρ_w (kg/m^3)	k_{rs}	k_{rw}	S_w	P_{ave} (psig)
Steam inlet	1.0000	0.0133	1.50	0.2127	934.31				
Water inlet	0.0000	0.0133	1.45	0.2146	935.19				
Port 1	0.9927	0.0133	1.45	0.2149	935.30				
Port 2	0.9981	0.0132	1.37	0.2185	936.90				
Port 3	1.0013	0.0131	1.29	0.2226	938.69	0.9607	0.0000	0.3094	20.94
Port 4	1.0107	0.0131	1.20	0.2275	940.78				
Port 5	1.0222	0.0130	1.11	0.2331	943.08				
Port 6	1.0215	0.0129	1.01	0.2399	945.66				
Port 7	1.0275	0.0127	0.90	0.2488	948.80	1.0779	0.0000	0.2884	12.16
Port 8	1.0303	0.0126	0.78	0.2594	952.12				
Outlet	1.0348	0.0124	0.66	0.2739	956.03				

Step 13

Position	Flowrate (cc/min)	Flowrate (kg/s)	Current (A)	Voltage (V)	Elec. Input (kJ/kg)
Steam line	3.7	6.17E-05	1.627	99.6	2627.82
Water line	2.3	3.83E-05	0.465	30	363.91

Position	Distance (cm)	P (psig)	P(abs) (psia)	T (^oC)	T_{sat} (^oC)	$h_s(P)$ (kJ/kg)	$h_w(P)$ (kJ/kg)	Q_{lost} (W/m^2)	Enthalpy (kJ/kg)
Steam inlet	0	27.53	42.23	136.83	132.90	2723	558		2723
Water inlet	0	26.37	41.07	106.75	132.01	2722	555		448
Port 1	3.5	26.15	40.85	131.39	131.84	2722	554	-152.83	1889
Port 2	8.5	23.75	38.45	125.46	129.84	2719	545	-88.15	1910
Port 3	13.5	21.18	35.88	128.87	127.50	2716	535	-82.11	1930
Port 4	18.5	18.37	33.07	126.98	124.71	2712	524	-106.51	1956
Port 5	23.5	15.41	30.11	118.50	121.49	2708	510	-150.95	1994
Port 6	28.5	12.28	26.98	115.42	117.79	2703	494	23.62	1988
Port 7	33.5	8.68	23.38	106.86	113.16	2697	475	-136.70	2021
Port 8	38.5	5.03	19.73	106.14	108.02	2689	453	-110.55	2048
Outlet	43.5	1.24	15.94	99.07	102.27	2680	429	-101.05	2061

Position	X	μ_s (cp)	ρ_s (kg/m^3)	μ_w (cp)	ρ_w (kg/m^3)	k_{rs}	k_{rw}	S_w	P_{ave} (psig)
Steam inlet	1.0000	0.0134	1.60	0.2082	932.26				
Water inlet	0.0000	0.0134	1.56	0.2098	933.02				
Port 1	0.6156	0.0134	1.55	0.2102	933.17				
Port 2	0.6278	0.0133	1.47	0.2139	934.84				
Port 3	0.6397	0.0132	1.38	0.2182	936.76	0.7603	0.0104	0.4019	23.66
Port 4	0.6547	0.0131	1.28	0.2233	939.02				
Port 5	0.6749	0.0130	1.17	0.2294	941.58				
Port 6	0.6761	0.0129	1.05	0.2368	944.49				
Port 7	0.6961	0.0128	0.92	0.2467	948.09	0.9164	0.0075	0.3772	13.53
Port 8	0.7135	0.0126	0.79	0.2591	952.02				
Outlet	0.7252	0.0124	0.65	0.2754	956.39				

Step 14

Position	Flowrate (cc/min)	Flowrate (kg/s)	Current (A)	Voltage (V)	Elec. Input (kJ/kg)
Steam line	3.6	6.00E-05	1.609	98.5	2641.44
Water line	0.4	6.67E-06	0.375	24.76	1392.75

Position	Distance (cm)	P (psig)	P(abs) (psia)	T (^oC)	T_{sat} (^oC)	$h_s(P)$ (kJ/kg)	$h_w(P)$ (kJ/kg)	Q_{lost} (W/m^2)	Enthalpy (kJ/kg)
Steam inlet	0	23.36	38.06	133.49	129.50	2719	544		2719
Water inlet	0	22.18	36.88	126.93	128.44	2717	539		533
Port 1	3.5	22.01	36.71	132.19	128.28	2717	539	-71.43	2526
Port 2	8.5	19.89	34.59	124.55	126.25	2714	530	-31.44	2538
Port 3	13.5	17.72	32.42	125.88	124.02	2711	521	-9.73	2542
Port 4	18.5	15.36	30.06	124.96	121.43	2708	510	-59.55	2564
Port 5	23.5	12.92	27.62	114.58	118.57	2704	498	-78.51	2592
Port 6	28.5	10.35	25.05	112.49	115.35	2700	484	-11.67	2597
Port 7	33.5	7.40	22.10	103.29	111.40	2694	467	-40.57	2612
Port 8	38.5	4.46	19.16	102.49	107.19	2688	449	-19.67	2619
Outlet	43.5	1.22	15.92	98.73	102.23	2679	428	-16.41	2622

Position	X	μ_s (cp)	ρ_s (kg/m^3)	μ_w (cp)	ρ_w (kg/m^3)	k_{rs}	k_{rw}	S_w	P_{ave} (psig)
Steam inlet	1.0000	0.0133	1.46	0.2145	935.12				
Water inlet	0.0000	0.0133	1.41	0.2164	936.00				
Port 1	0.9125	0.0132	1.41	0.2167	936.12				
Port 2	0.9193	0.0132	1.33	0.2205	937.78				
Port 3	0.9225	0.0131	1.25	0.2246	939.57	0.9221	0.0018	0.3281	19.87
Port 4	0.9343	0.0130	1.17	0.2295	941.63				
Port 5	0.9493	0.0129	1.08	0.2352	943.88				
Port 6	0.9535	0.0128	0.98	0.2419	946.39				
Port 7	0.9629	0.0127	0.87	0.2507	949.44	1.0799	0.0008	0.3004	11.38
Port 8	0.9692	0.0125	0.77	0.2612	952.65				
Outlet	0.9744	0.0124	0.64	0.2755	956.42				

Step 15

Position	Flowrate (cc/min)	(kg/s)	Current (A)	Voltage (V)	Elec. Input (kJ/kg)
Steam line	3.5	5.83E-05	1.605	98.17	2701.08
Water line	0.5	8.33E-06	0.34	23.4	954.72

Position	Distance (cm)	P (psig)	P(abs) (psia)	T (^oC)	T_{sat} (^oC)	$h_s(P)$ (kJ/kg)	$h_w(P)$ (kJ/kg)	Q_{lost} (W/m^2)	Enthalpy (kJ/kg)
Steam inlet	0	23.27	37.97	148.59	129.42	2719	544		2719
Water inlet	0	22.10	36.80	124.89	128.37	2717	539		525
Port 1	3.5	21.88	36.58	130.76	128.16	2717	538	69.88	2419
Port 2	8.5	19.77	34.47	126.68	126.13	2714	530	73.19	2392
Port 3	13.5	17.61	32.31	126.41	123.91	2711	520	60.91	2369
Port 4	18.5	15.27	29.97	122.82	121.33	2708	509	61.42	2346
Port 5	23.5	12.83	27.53	114.67	118.47	2704	497	52.93	2327
Port 6	28.5	10.28	24.98	112.65	115.27	2700	484	42.81	2311
Port 7	33.5	7.35	22.05	103.98	111.33	2694	467	16.13	2305
Port 8	38.5	4.44	19.14	103.29	107.16	2688	449	9.40	2302
Outlet	43.5	1.22	15.92	98.65	102.23	2679	428	-3.51	2302

Position	X	μ_s (cp)	ρ_s (kg/m^3)	μ_w (cp)	ρ_w (kg/m^3)	k_{rs}	k_{rw}	S_w	P_{ave} (psig)
Steam inlet	1.0000	0.0133	1.45	0.2146	935.19				
Water inlet	0.0000	0.0133	1.41	0.2166	936.05				
Port 1	0.8631	0.0132	1.40	0.2169	936.23				
Port 2	0.8523	0.0132	1.33	0.2207	937.87				
Port 3	0.8438	0.0131	1.25	0.2248	939.66	0.8504	0.0036	0.3363	19.74
Port 4	0.8356	0.0130	1.16	0.2297	941.71				
Port 5	0.8291	0.0129	1.07	0.2354	943.96				
Port 6	0.8247	0.0128	0.98	0.2421	946.45				
Port 7	0.8254	0.0127	0.87	0.2509	949.49	0.9320	0.0036	0.3055	11.31
Port 8	0.8276	0.0125	0.76	0.2613	952.68				
Outlet	0.8325	0.0124	0.64	0.2755	956.41				

Step 16

Position	Flowrate (cc/min)	(kg/s)	Current (A)	Voltage (V)	Elec. Input (kJ/kg)
Steam line	3	5.00E-05	1.514	92.6	2803.93
Water line	1	1.67E-05	0.382	25.25	578.73

Position	Distance (cm)	P (psig)	P(abs) (psia)	T (^oC)	T_{sat} (^oC)	$h_s(P)$ (kJ/kg)	$h_w(P)$ (kJ/kg)	Q_{lost} (W/m^2)	Enthalpy (kJ/kg)
Steam inlet	0	22.43	37.13	150.15	128.67	2718	540		2718
Water inlet	0	21.29	35.99	116.39	127.61	2716	536		488
Port 1	3.5	21.14	35.84	126.58	127.46	2716	535	48.77	2142
Port 2	8.5	19.07	33.77	123.71	125.43	2713	527	55.74	2122
Port 3	13.5	16.93	31.63	124.13	123.17	2710	517	35.41	2109
Port 4	18.5	14.58	29.28	122.35	120.54	2707	506	51.21	2090
Port 5	23.5	12.12	26.82	112.77	117.59	2703	493	40.70	2075
Port 6	28.5	9.54	24.24	111.46	114.29	2698	479	27.10	2065
Port 7	33.5	6.59	21.29	104.02	110.27	2693	462	44.02	2049
Port 8	38.5	3.66	18.36	102.74	105.99	2686	444	17.28	2042
Outlet	43.5	0.50	15.20	97.22	101.09	2677	424	30.15	2037

Position	X	μ_s (cp)	ρ_s (kg/m^3)	μ_w (cp)	ρ_w (kg/m^3)	k_{rs}	k_{rw}	S_w	P_{ave} (psig)
Steam inlet	1.0000	0.0133	1.42	0.2160	935.81				
Water inlet	0.0000	0.0132	1.38	0.2180	936.68				
Port 1	0.7369	0.0132	1.38	0.2182	936.80				
Port 2	0.7295	0.0132	1.30	0.2220	938.44				
Port 3	0.7257	0.0131	1.22	0.2262	940.25	0.7553	0.0064	0.3612	19.03
Port 4	0.7197	0.0130	1.14	0.2313	942.33				
Port 5	0.7157	0.0129	1.05	0.2372	944.65				
Port 6	0.7145	0.0128	0.95	0.2442	947.21	0.7793	0.0060	0.3422	12.06
Port 7	0.7113	0.0127	0.84	0.2534	950.31	0.7404	0.0053	0.3269	8.07
Port 8	0.7129	0.0125	0.74	0.2645	953.57				
Outlet	0.7157	0.0123	0.62	0.2792	957.28				

Step 17

Position	Flowrate (cc/min)	Flowrate (kg/s)	Current (A)	Voltage (V)	Elec. Input (kJ/kg)
Steam line	3	5.00E-05	1.433	87.62	2511.19
Water line	2	3.33E-05	0.385	25.4	293.37

Position	Distance (cm)	P (psig)	P(abs) (psia)	T (^oC)	T_{sat} (^oC)	$h_s(P)$ (kJ/kg)	$h_w(P)$ (kJ/kg)	Q_{lost} (W/m^2)	Enthalpy (kJ/kg)
Steam inlet	0	22.61	37.31	124.70	128.83	2718	541		2678
Water inlet	0	21.50	36.20	100.86	127.80	2716	537		423
Port 1	3.5	21.35	36.05	129.59	127.67	2716	536	39.78	1764
Port 2	8.5	19.24	33.94	125.74	125.60	2713	527	50.00	1750
Port 3	13.5	17.01	31.71	125.24	123.26	2710	517	40.47	1738
Port 4	18.5	14.59	29.29	123.03	120.55	2707	506	80.20	1714
Port 5	23.5	12.09	26.79	113.78	117.56	2703	493	31.06	1705
Port 6	28.5	9.43	24.13	111.99	114.15	2698	479	77.43	1682
Port 7	33.5	6.41	21.11	104.42	110.02	2692	461	4.35	1681
Port 8	38.5	3.42	18.12	102.86	105.63	2685	443	-0.43	1681
Outlet	43.5	0.34	15.04	98.24	100.82	2677	422	-14.54	1683

Position	X	μ_s (cp)	ρ_s (kg/m^3)	μ_w (cp)	ρ_w (kg/m^3)	k_{rs}	k_{rw}	S_w	P_{ave} (psig)
Steam inlet	1.0000	0.0133	1.43	0.2157	935.67				
Water inlet	0.0000	0.0132	1.39	0.2176	936.52				
Port 1	0.5634	0.0132	1.38	0.2179	936.63				
Port 2	0.5591	0.0132	1.31	0.2217	938.31				
Port 3	0.5564	0.0131	1.23	0.2260	940.18	0.7001	0.0126		19.18
Port 4	0.5489	0.0130	1.14	0.2312	942.32				
Port 5	0.5483	0.0129	1.05	0.2372	944.67				
Port 6	0.5421	0.0128	0.95	0.2445	947.32	0.7246	0.0117		12.01
Port 7	0.5466	0.0127	0.84	0.2541	950.50	0.7005	0.0103		7.92
Port 8	0.5521	0.0125	0.73	0.2655	953.84				
Outlet	0.5591	0.0123	0.61	0.2801	957.48				

Step 18

Position	Flowrate (cc/min)	Flowrate (kg/s)	Current (A)	Voltage (V)	Elec. Input (kJ/kg)
Steam line	3	5.00E-05	1.437	88	2529.12
Water line	2.5	4.17E-05	0.47	30.6	345.17

Position	Distance (cm)	P (psig)	P(abs) (psia)	T (^oC)	T_{sat} (^oC)	$h_s(P)$ (kJ/kg)	$h_w(P)$ (kJ/kg)	Q_{lost} (W/m^2)	Enthalpy (kJ/kg)
Steam inlet	0	23.99	38.69	124.30	130.05	2719	546		2696
Water inlet	0	22.86	37.56	102.72	129.05	2718	542		431
Port 1	3.5	22.59	37.29	131.78	128.82	2718	541	69.98	1648
Port 2	8.5	20.38	35.08	128.18	126.73	2715	532	74.57	1628
Port 3	13.5	18.00	32.70	123.63	124.32	2712	522	62.58	1611
Port 4	18.5	15.42	30.12	122.89	121.50	2708	510	122.07	1578
Port 5	23.5	12.72	27.42	114.96	118.33	2704	497	53.03	1564
Port 6	28.5	9.88	24.58	109.22	114.74	2699	481	43.84	1552
Port 7	33.5	6.67	21.37	105.59	110.38	2693	463	17.34	1548
Port 8	38.5	3.47	18.17	103.19	105.71	2685	443	4.75	1546
Outlet	43.5	0.22	14.92	98.39	100.64	2677	422	-8.36	1547

Position	X	μ_s (cp)	ρ_s (kg/m^3)	μ_w (cp)	ρ_w (kg/m^3)	k_{rs}	k_{rw}	S_w	P_{ave} (psig)
Steam inlet	1.0000	0.0133	1.48	0.2135	934.67				
Water inlet	0.0000	0.0133	1.44	0.2153	935.49				
Port 1	0.5084	0.0133	1.43	0.2157	935.69				
Port 2	0.5019	0.0132	1.35	0.2196	937.39				
Port 3	0.4973	0.0131	1.26	0.2241	939.34	0.6335	0.0147	0.4293	20.30
Port 4	0.4859	0.0130	1.17	0.2294	941.57				
Port 5	0.4836	0.0129	1.07	0.2357	944.07				
Port 6	0.4829	0.0128	0.97	0.2432	946.87	0.6505	0.0135	0.4129	12.65
Port 7	0.4864	0.0127	0.85	0.2532	950.22	0.6381	0.0120	0.3949	8.27
Port 8	0.4920	0.0125	0.73	0.2652	953.78				
Outlet	0.4992	0.0123	0.61	0.2807	957.62				

Step 19

Position	Flowrate (cc/min)	Flowrate (kg/s)	Current (A)	Voltage (V)	Elec. Input (kJ/kg)
Steam line	2.5	4.17E-05	1.24	75.24	2239.14
Water line	3	5.00E-05	0.471	30.54	287.69

Position	Distance (cm)	P (psig)	P(abs) (psia)	T (^oC)	T_{sat} (^oC)	$h_s(P)$ (kJ/kg)	$h_w(P)$ (kJ/kg)	Q_{lost} (W/m^2)	Enthalpy (kJ/kg)
Steam inlet	0	19.90	34.60	120.15	126.26	2714	530		2406
Water inlet	0	18.69	33.39	97.61	125.04	2713	525		409
Port 1	3.5	18.51	33.21	127.55	124.85	2712	524	41.90	1306
Port 2	8.5	16.67	31.37	124.01	122.89	2710	516	30.33	1297
Port 3	13.5	14.69	29.39	120.38	120.66	2707	506	25.66	1291
Port 4	18.5	12.57	27.27	118.06	118.14	2704	496	78.93	1269
Port 5	23.5	10.35	25.05	111.32	115.35	2700	484	32.35	1261
Port 6	28.5	8.07	22.77	108.91	112.32	2696	471	36.76	1251
Port 7	33.5	5.44	20.14	103.18	108.62	2690	455	-31.89	1259
Port 8	38.5	2.85	17.55	101.74	104.77	2684	439	-4.13	1261
Outlet	43.5	0.21	14.91	96.71	100.62	2677	422	-14.73	1263

Position	X	μ_s (cp)	ρ_s (kg/m^3)	μ_w (cp)	ρ_w (kg/m^3)	k_{rs}	k_{rw}	S_w	P_{ave} (psig)
Steam inlet	1.0000	0.0132	1.33	0.2204	937.77				
Water inlet	0.0000	0.0131	1.29	0.2227	938.76				
Port 1	0.3571	0.0131	1.28	0.2231	938.91				
Port 2	0.3562	0.0131	1.21	0.2267	940.47				
Port 3	0.3564	0.0130	1.14	0.2310	942.24	0.5985	0.0233	0.4697	16.60
Port 4	0.3504	0.0129	1.06	0.2361	944.21				
Port 5	0.3506	0.0128	0.98	0.2419	946.39				
Port 6	0.3506	0.0127	0.90	0.2486	948.73	0.6212	0.0213	0.4438	10.32
Port 7	0.3598	0.0126	0.80	0.2575	951.56	0.6062	0.0186	0.4123	6.75
Port 8	0.3659	0.0125	0.71	0.2679	954.50				
Outlet	0.3729	0.0123	0.61	0.2807	957.63				

Step 20

Position	Flowrate (cc/min)	Flowrate (kg/s)	Current (A)	Voltage (V)	Elec. Input (kJ/kg)
Steam line	1.5	2.50E-05	0.992	60	2380.80
Water line	3.5	5.83E-05	0.527	34	307.17

Position	Distance (cm)	P (psig)	P(abs) (psia)	T (^oC)	T_{sat} (^oC)	$h_s(P)$ (kJ/kg)	$h_w(P)$ (kJ/kg)	Q_{lost} (W/m^2)	Enthalpy (kJ/kg)
Steam inlet	0	15.37	30.07	117.90	121.44	2708	510		2548
Water inlet	0	14.31	29.01	96.58	120.23	2706	505		405
Port 1	3.5	14.29	28.99	124.65	120.20	2706	504	39.79	1036
Port 2	8.5	12.83	27.53	117.24	118.46	2704	497	43.68	1023
Port 3	13.5	11.25	25.95	117.03	116.50	2701	489	28.32	1015
Port 4	18.5	9.58	24.28	107.03	114.34	2698	480	-19.95	1021
Port 5	23.5	7.86	22.56	107.03	112.03	2695	470	35.73	1010
Port 6	28.5	6.17	20.87	106.06	109.67	2692	460	31.74	1001
Port 7	33.5	4.13	18.83	101.74	106.70	2687	447	11.65	997
Port 8	38.5	2.26	16.96	98.19	103.86	2682	435	-3.33	998
Outlet	43.5	0.30	15.00	97.18	100.77	2677	422	-13.64	1000

Position	X	μ_s (cp)	ρ_s (kg/m^3)	μ_w (cp)	ρ_w (kg/m^3)	k_{rs}	k_{rw}	S_w	P_{ave} (psig)
Steam inlet	1.0000	0.0130	1.17	0.2295	941.62				
Water inlet	0.0000	0.0130	1.13	0.2319	942.58				
Port 1	0.2413	0.0130	1.13	0.2319	942.60				
Port 2	0.2383	0.0129	1.07	0.2354	943.97				
Port 3	0.2377	0.0129	1.02	0.2394	945.49	0.5066	0.0325	0.4905	12.77
Port 4	0.2438	0.0128	0.95	0.2441	947.17				
Port 5	0.2427	0.0127	0.89	0.2493	948.95				
Port 6	0.2423	0.0126	0.83	0.2549	950.76				
Port 7	0.2455	0.0125	0.75	0.2625	953.03	0.5764	0.0293	0.4675	6.85
Port 8	0.2505	0.0124	0.68	0.2705	955.18				
Outlet	0.2564	0.0123	0.61	0.2803	957.52				

Step 21

Position	Flowrate (cc/min)	(kg/s)	Current (A)	Voltage (V)	Elec. Input (kJ/kg)
Steam line	0.5	8.33E-06	0.538	32.54	2100.78
Water line	4.5	7.50E-05	0.646	40.5	348.84

Position	Distance (cm)	P (psig)	P(abs) (psia)	T (^oC)	T_{sat} (^oC)	$h_s(P)$ (kJ/kg)	$h_w(P)$ (kJ/kg)	Q_{lost} (W/m^2)	Enthalpy (kJ/kg)
Steam inlet	0	6.73	21.43	109.03	110.46	2693	463		2258
Water inlet	0	5.92	20.62	94.96	109.32	2691	458		398
Port 1	3.5	6.19	20.89	116.63	109.69	2692	460	50.40	569
Port 2	8.5	5.29	19.99	109.81	108.41	2690	455	51.26	554
Port 3	13.5	4.67	19.37	106.78	107.50	2688	451	45.76	540
Port 4	18.5	3.99	18.69	105.37	106.49	2687	446	27.16	532
Port 5	23.5	3.34	18.04	101.37	105.51	2685	442	52.10	517
Port 6	28.5	2.75	17.45	101.00	104.61	2684	439	73.98	495
Port 7	33.5	1.97	16.67	98.60	103.40	2682	433	32.90	486
Port 8	38.5	1.22	15.92	99.09	102.23	2679	428	29.18	477
Outlet	43.5	0.28	14.98	92.28	100.73	2677	422	20.14	474

Position	X	μ_s (cp)	ρ_s (kg/m^3)	μ_w (cp)	ρ_w (kg/m^3)	k_{rs}	k_{rw}	S_w	P_{ave} (psig)
Steam inlet	1.0000	0.0127	0.85	0.2530	950.16				
Water inlet	0.0000	0.0126	0.82	0.2558	951.03				
Port 1	0.0488	0.0126	0.83	0.2548	950.74				
Port 2	0.0444	0.0126	0.80	0.2581	951.73				
Port 3	0.0401	0.0126	0.77	0.2604	952.42	0.2686	0.1083	0.6342	4.98
Port 4	0.0384	0.0125	0.75	0.2631	953.18				
Port 5	0.0333	0.0125	0.72	0.2658	953.93				
Port 6	0.0253	0.0124	0.70	0.2683	954.61	0.1849	0.1111	0.6130	3.37
Port 7	0.0232	0.0124	0.67	0.2719	955.53	0.1398	0.0893	0.6342	2.36
Port 8	0.0215	0.0124	0.64	0.2755	956.41				
Outlet	0.0230	0.0123	0.61	0.2804	957.55				

Step 22

Position	Flowrate (cc/min)	Flowrate (kg/s)	Current (A)	Voltage (V)	Elec. Input (kJ/kg)
Steam line	1	1.67E-05	0.58	35.1	1221.48
Water line	4	6.67E-05	0.644	40.4	390.26

Position	Distance (cm)	P (psig)	P(abs) (psia)	T (^oC)	T_{sat} (^oC)	$h_s(P)$ (kJ/kg)	$h_w(P)$ (kJ/kg)	Q_{lost} (W/m^2)	Enthalpy (kJ/kg)
Steam inlet	0	8.88	23.58	111.43	113.41	2697	476		1388
Water inlet	0	8.07	22.77	102.25	112.32	2696	471		429
Port 1	3.5	8.02	22.72	118.80	112.26	2695	471	-54.42	637
Port 2	8.5	7.33	22.03	113.75	111.31	2694	467	-17.91	642
Port 3	13.5	6.58	21.28	110.27	110.25	2692	462	-11.56	645
Port 4	18.5	5.70	20.40	107.01	108.99	2691	457	-15.78	650
Port 5	23.5	4.88	19.58	103.63	107.80	2689	452	-45.48	663
Port 6	28.5	4.06	18.76	103.01	106.60	2687	447	-12.25	667
Port 7	33.5	2.95	17.65	99.48	104.91	2684	440	-48.53	681
Port 8	38.5	1.78	16.48	100.49	103.10	2681	432	-30.34	690
Outlet	43.5	0.33	15.03	95.80	100.81	2677	422	-35.85	695

Position	X	μ_s (cp)	ρ_s (kg/m^3)	μ_w (cp)	ρ_w (kg/m^3)	k_{rs}	k_{rw}	S_w	P_{ave} (psig)
Steam inlet	1.0000	0.0128	0.93	0.24613	947.89				
Water inlet	0.0000	0.0127	0.90	0.24861	948.73				
Port 1	0.0745	0.0127	0.90	0.24875	948.78				
Port 2	0.0786	0.0127	0.87	0.25096	949.51				
Port 3	0.0820	0.0127	0.84	0.25348	950.32	0.4178	0.0831565	0.6026	6.96
Port 4	0.0864	0.0126	0.81	0.25659	951.28				
Port 5	0.0945	0.0126	0.78	0.25962	952.19				
Port 6	0.0982	0.0125	0.75	0.26282	953.11	0.5141	0.0766618	0.5779	4.88
Port 7	0.1076	0.0125	0.71	0.26749	954.38	0.4344	0.0564793	0.5438	3.50
Port 8	0.1148	0.0124	0.67	0.27282	955.76				
Outlet	0.1211	0.0123	0.61	0.28009	957.48				

Step 23

Position	Flowrate (cc/min)	Flowrate (kg/s)	Current (A)	Voltage (V)	Elec. Input (kJ/kg)
Steam line	2.5	4.17E-05	0.369	24.1	213.43
Water line	2.5	4.17E-05	25.5	0.423	258.88

Position	Distance (cm)	P (psig)	P(abs) (psia)	T (^oC)	T_{sat} (^oC)	$h_s(P)$ (kJ/kg)	$h_w(P)$ (kJ/kg)	Q_{lost} (W/m^2)	Enthalpy (kJ/kg)
Steam inlet	0	1.10	15.80	68.91	102.04	2679	428		288.47
Water inlet	0	0.46	15.16	55.23	101.02	2677	423		231.21
Port 1	3.5	1.15	15.85	71.31	102.12	2679	428	-73.37	281.46
Port 2	8.5	1.04	15.74	70.27	101.94	2679	427	-60.64	299.34
Port 3	13.5	0.82	15.52	73.37	101.59	2678	426	-61.08	317.34
Port 4	18.5	0.63	15.33	85.94	101.29	2678	424	-36.95	328.23
Port 5	23.5	0.52	15.22	84.70	101.11	2677	424	-24.50	335.45
Port 6	28.5	0.42	15.12	86.45	100.96	2677	423	-26.10	343.14
Port 7	33.5	0.26	14.96	86.01	100.70	2677	422	-38.34	354.44
Port 8	38.5	0.38	15.08	88.02	100.89	2677	423	-26.71	362.31
Outlet	43.5	0.24	14.94	86.37	100.66	2677	422	-29.91	366.72

Position	X	μ_s (cp)	ρ_s (kg/m^3)	μ_w (cp)	ρ_w (kg/m^3)	k_{rs}	k_{rw}	S_w	P_{ave} (psig)
Steam inlet	1.0000	0.01235	0.64	0.2761	956.56				
Water inlet	0.0000	0.01230	0.62	0.2794	957.33				
Port 1	0.0000	0.01235	0.64	0.2759	956.50				
Port 2	0.0000	0.01234	0.64	0.2764	956.63	0.0000	0.6727	0.9514	1.10
Port 3	0.0000	0.01233	0.63	0.2776	956.90				
Port 4	0.0000	0.01232	0.62	0.2785	957.12				
Port 5	0.0000	0.01231	0.62	0.2791	957.26				
Port 6	0.0000	0.01230	0.61	0.2796	957.38	0.0000	0.7080	0.9159	0.53
Port 7	0.0000	0.01229	0.61	0.2805	957.57				
Port 8	0.0000	0.01230	0.61	0.2798	957.43				
Outlet	0.0000	0.01229	0.61	0.2806	957.60				

Appendix C : Correction for Slip Effect

b = 6.58 psia

Step No.	S_w	K_{rs}	K_{rw}	P_{av} (psia)	$K_{rs,corr}/K_{rs}$	$K_{rs,\ corr}$
1	0.799	0.025	0.489	19.874	0.75	0.019
	0.764	0.059	0.425	18.075	0.73	0.043
	0.715	0.087	0.319	17.857	0.73	0.063
	0.682	0.116	0.274	16.877	0.72	0.083
3	0.621	0.189	0.113	19.740	0.75	0.141
	0.689	0.000	0.190	16.534	0.71	0.000
	0.978	0.000	0.744	15.475	0.70	0.000
4	0.593	0.180	0.080	26.945	0.80	0.144
	0.555	0.140	0.066	24.951	0.79	0.110
	0.526	0.130	0.059	23.304	0.78	0.101
	0.489	0.158	0.043	18.964	0.74	0.117
5	0.568	0.252	0.068	24.779	0.79	0.198
	0.587	0.240	0.069	22.845	0.77	0.186
	0.572	0.311	0.077	19.040	0.74	0.230
6	0.520	0.376	0.038	30.904	0.82	0.309
	0.501	0.417	0.034	24.788	0.79	0.329
7	0.484	0.489	0.024	33.595	0.83	0.408
	0.460	0.600	0.020	25.043	0.79	0.474
8	0.463	0.431	0.019	33.639	0.83	0.360
	0.438	0.536	0.016	24.980	0.79	0.423
9	0.400	0.474	0.010	36.678	0.85	0.401
	0.375	0.532	0.009	26.835	0.80	0.426
10	0.340	0.779	0.003	34.393	0.84	0.652
	0.315	0.840	0.003	28.202	0.81	0.679
	0.291	0.900	0.003	22.574	0.77	0.695
11	0.323	0.965	0.000	34.369	0.84	0.808
	0.302	1.044	0.000	28.237	0.81	0.844
12	0.309	0.961	0.000	35.642	0.84	0.809
	0.288	1.078	0.000	26.856	0.80	0.863
13	0.402	0.760	0.010	38.363	0.852	0.648
	0.377	0.916	0.008	28.230	0.809	0.741
14	0.328	0.922	0.002	34.565	0.838	0.773
	0.300	1.080	0.001	26.079	0.796	0.860
15	0.336	0.850	0.004	34.444	0.838	0.712
	0.306	0.932	0.004	26.010	0.796	0.742
16	0.361	0.755	0.006	33.731	0.835	0.630
	0.342	0.779	0.006	26.761	0.800	0.624
	0.327	0.740	0.005	22.765	0.773	0.572
17	0.421	0.700	0.013	33.882	0.835	0.585
	0.403	0.725	0.012	26.711	0.800	0.580
	0.421	0.700	0.010	22.621	0.772	0.541
18	0.429	0.633	0.015	34.995	0.840	0.532
	0.413	0.651	0.013	27.349	0.804	0.523
	0.395	0.638	0.012	22.971	0.775	0.494
19	0.470	0.598	0.023	31.297	0.824	0.493
	0.444	0.621	0.021	25.018	0.789	0.490
	0.412	0.606	0.019	21.454	0.763	0.462
20	0.491	0.507	0.032	27.472	0.804	0.408
	0.468	0.576	0.029	21.553	0.763	0.440
21	0.634	0.269	0.108	19.680	0.747	0.201
	0.613	0.185	0.111	18.073	0.730	0.135
	0.634	0.140	0.089	17.060	0.719	0.100
22	0.603	0.418	0.083	21.657	0.764	0.319
	0.578	0.514	0.077	19.579	0.746	0.383
	0.544	0.434	0.056	18.205	0.732	0.318
23	0.951	0.000	0.673	15.795	0.703	0.000
	0.916	0.000	0.708	15.227	0.695	0.000